Effect of Polyelectrolyte Adsorption on Intercolloidal Forces

Itamar Borukhov,[†] David Andelman,*,[†] and Henri Orland[‡]

School of Physics and Astronomy, Raymond and Beverly Sackler Faculty of Exact Sciences, Tel-Aviv University, Ramat-Aviv 69978, Tel-Aviv, Israel, and Service de Physique Théorique, CE-Saclay, 91191 Gif-sur-Yvette Cedex, France

Received: January 5, 1999§

The behavior of polyelectrolytes between charged surfaces immersed in semidilute solutions is investigated theoretically. A continuum mean field approach is used for calculating numerically concentration profiles between two electrodes held at a constant potential. A generalized contact theorem relates the intersurface forces to the concentration profiles. The numerical results show that overcompensation of the surface charges by adsorbing polyelectrolytes can lead to effective *attraction* between *equally charged* surfaces. Simple scaling arguments enable us to characterize qualitatively the intersurface interactions as a function of the fraction of charged monomers p and the salt concentration c_b. In the low-salt regime, we find strong repulsion at short distances, where the polymers are depleted from the intersurface gap, followed by strong attraction when the two adsorbed layers overlap. The magnitude of this attraction scales as $p^{1/2}$ and its dominant length scale is proportional to $a/p^{1/2}$, where a is the monomer size. At larger distances, the two adsorbing surfaces interact via a weak electrostatic repulsion. For strong polyelectrolytes at high salt concentration, the polymer contribution to attraction at short distances scales as $p/c_s^{1/2}$ and the length scale is proportional to $\kappa_s a^2/p$, where κ_s^{-1} is the Debye−Hückel screening length. For weak polyelectrolytes at high salt concentration, the interaction is repulsive for all surface separations and decays exponentially with a decay length equal to κ_s^{-1}. The effect of irreversible adsorption is discussed as well, and it is shown that intersurface attraction can be obtained in this case as well.

I. Introduction

Polymers are known to affect the interactions of colloidal particles in solution.[1−3] Adsorption of charged polymers (*polyelectrolytes*) to oppositely charged colloids may turn intercolloidal repulsion into attraction, leading to flocculation. This phenomenon is used in industrial applications such as water filtration, paper making, and mineral processing. The reversed process is useful as well, since adsorbed polyelectrolytes (in different conditions) can also stabilize colloidal suspensions such as paint, ink, or medical suspensions against attractive forces (e.g., van der Waals forces).

One of the most common techniques to study experimentally the adsorption of polyelectrolytes between two surfaces is the surface force apparatus (SFA),[4] which allows delicate measurements of inter-surface forces at distances as small as a few angstroms. In these experiments,[5−12] attractive and repulsive forces have been observed, depending on specific details, such as the type of polyelectrolyte, its concentration, the ionic strength of the solution, etc. Using other experimental techniques it was possible to measure the disjoining pressure of thin liquid films in the presence of polyelectrolytes and as a function of the film width.[13] Both repulsive and attractive forces have been measured using this method.

Adsorption of polyelectrolytes was treated theoretically in a discrete model,[14−17] where the thermodynamic state of the system is described by occupation fractions of monomers, ions, and solvent molecules on a discrete lattice. Within mean field theory, the equilibrium state of the system corresponds to the

maximal contribution to the partition function of the system and can be calculated numerically. Böhmer et al.[18] have used this model to calculate force curves at relatively short distances (up to 30 molecular layers). In addition, Monte Carlo computer simulations of polyelectrolytes between flat surfaces[19] and between charged spheres[20] provide valuable hints concerning the complex behavior of polyelectrolytes. However, they are limited to relatively short chains and small intersurface distances due to computation time limitations.

Another theoretical approach is a continuum one[21−28] where the concentration of the different species are taken to be continuous functions of the spatial coordinates. The mean-field equation of state can be calculated by solving two differential equations for the polymer concentration and the electrostatic potential derived using a variational procedure. Varoqui et al.[22,23] used the continuum approach to investigate polyelectrolyte adsorption onto one surface, while Podgornik[27] used a similar formalism to calculate intersurface forces. In those works, the nonlinear excluded volume interaction between the monomers has not been considered. Châtellier and Joanny[28] used a linearized version of a similar approach to study the intersurface forces for polyelectrolytes in a poor solvent. Recently, we have been able to derive some simple scaling relations for the adsorption of polyelectrolytes onto a single charged surface.[26] These scaling relations were compared to the exact numerical solutions of the differential equations and to existing experimental results. The agreement was reasonable in two opposite limits, (i) low salt concentration (no electrostatic screening), and (ii) high salt concentration (strong screening).

In the present work, the continuum mean-field model is used to study polyelectrolyte adsorption between two parallel surfaces. The advantage of our model is that the connectivity of the polymer chains, the excluded volume repulsion between
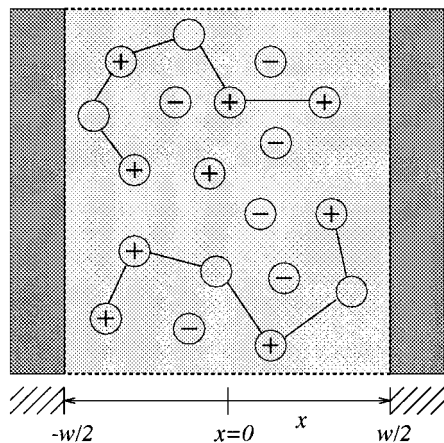
Figure 1. Schematic view of a polyelectrolyte solution between two parallel charged surfaces at a distance w from each other. The solution contains polyelectrolyte chains and small ions. The surfaces are kept at a constant potential.

monomers in a good solvent, and the Coulomb interactions between the charged monomers, counterions, co-ions and surface charges are all taken into account. However, the approximations involved neglect charge fluctuations, ion–ion correlations, ionic finite size and the stiffening of the charged chains. The mean-field equations are solved numerically in order to obtain concentration profiles, and the intersurface forces are then calculated from the free energy. In addition, we extend our earlier scaling approach of one adsorbing surface[26] to the case of two interacting surfaces. A qualitative description of the intersurface forces as a function of the polyelectrolyte charge and the amount of salt in the solution is obtained.

The paper is organized as follows. In the next section we describe the mean-field approach. In section III, we present numerical results obtained from solving the mean-field equations, and in section IV, we use simple scaling arguments to describe the intersurface forces. In section V, we study the effect of irreversible adsorption both numerically and analytically, and in section VI, we compare our results with experiments.

II. Mean-Field Approach

A. Basic Equations. The model system consists of a semidilute solution of polyelectrolytes in a good solvent placed between two flat surfaces (Figure 1). The solution contains charged polymer chains, counterions, and a monovalent electrolyte (salt). Having in mind the experimental setup of the surface force apparatus (SFA) discussed below, we consider a system which is coupled to a bulk reservoir of polyelectrolyte chains and salt.

As discussed elsewhere,[24,25] the charge distribution along the chains depends on the type of polyelectrolyte as well as on the local conditions, such as the pH and the electrostatic potential. However, at low electrostatic potentials $|\beta e\psi| \ll 1$, where ψ is the electrostatic potential, $\beta = 1/k_BT$ the inverse thermal energy, and e the electron charge, the differences between the various charge distribution models are small. We assume hereafter the simplest case of a uniform ("smeared") charge distribution along the polymer chains with a fractional charge pe attached to each monomer.

In the mean-field approach, the free energy of the system is expressed in terms of the local electrostatic potential $\psi(\mathbf{r})$ at a point $\mathbf{r}$ and the polymer order parameter $\phi(\mathbf{r})$ which is related to the local monomer concentration through $c_m(\mathbf{r}) = |\phi(\mathbf{r})|^2$. The relation between the polymer order parameter and the monomer concentration is analogous to the relation between

the wave function and the probability density of a particle in quantum mechanics. The excess free energy with respect to the bulk can be divided into three contributions:[22-25]

$$F = \int f(\mathbf{r})\, d\mathbf{r} = \int \left\{ f_{pol}(\mathbf{r}) + f_{ions}(\mathbf{r}) + f_{el}(\mathbf{r}) \right\} d\mathbf{r} \quad (1)$$

The polymer contribution is

$$f_{pol}(\mathbf{r}) = k_BT \left[\frac{a^2}{6} |\nabla\phi|^2 + \frac{1}{2}\upsilon(\phi^4 - \phi_b{}^4) \right] - \mu_p(\phi^2 - \phi_b{}^2) \quad (2)$$

where the first term is the polymer response to local variations of the concentration and is due to the connectivity of the polymer chain, a being the effective monomer size. The second term represents the short-range monomer–monomer interaction and can be viewed as representing an effective volume of a single monomer. For polymers in a good solvent, υ is positive. However, since υ represents an *effective* monomer–monomer interaction, it can also be negative (in a poor solvent) or zero (in a θ solvent) requiring higher order terms in ϕ^2 to be included in the free energy. For simplicity we will limit ourselves to good solvent conditions but the formalism can be easily generalized to other conditions as well. The last term couples the system to a reservoir, μ_p being the polymer chemical potential and $\phi_b{}^2$ the bulk monomer concentration.

The nonelectrostatic contribution of the small (monovalent) ions is due to their translation entropy and is equal to

$$f_{ions}(\mathbf{r}) = \sum_{i=\pm} \left\{ k_BT \left[c^i \ln c^i - c^i - (c_b^i \ln c_b^i - c_b^i) \right] - \mu^i(c^i - c_b^i) \right\} \quad (3)$$

where $c^i(\mathbf{r})$ is the local concentration of the $i = \pm$ ions (cations and anions) and c_b^i, μ^i are the bulk concentration and chemical potential, respectively. In the most general case, the solution contains two types of negative ions, the counterions which dissociate from the polymer chains and the salt anions. In the reservoir, the concentration of negative ions has two contributions $c_b{}^- = c_b + p\phi_b{}^2$ where c_b is the electrolyte bulk concentration, while for the positive ions $c_b{}^+ = c_b$. In principle, one could consider the two types of negative ions separately, but for clarity we take the two types of negative ions to be identical.

Finally, the electrostatic contribution is

$$f_{el}(\mathbf{r}) = pe\phi^2\psi + ec^+\psi - ec^-\psi - \frac{\epsilon}{8\pi}|\nabla\psi|^2 \quad (4)$$

The first term is the electrostatic energy of charged monomers. The next two terms represent the positive and negative ions, respectively, and the last term is the self-energy of the electric field where ϵ is the dielectric constant of the solution. The sum of the electrostatic contributions can be integrated by parts using the Poisson equation (derived below) and yields $F_{el} = (\epsilon/8\pi) \int |\nabla\psi|^2\, d\mathbf{r}$, as expected, plus electrostatic surface terms.

Minimization of the free energy with respect to $c^\pm$, ϕ, and ψ yields a Boltzmann distribution for the concentration of the small ions, $c^\pm(\mathbf{r}) = c_b^\pm \exp(\mp\beta e\psi)$, and two coupled differential equations[25] for ϕ and ψ with $\mu_p = k_BT\upsilon\phi_b{}^2$ and $\mu^i = k_BT \log c_b^i$:

$$\nabla^2\psi(\mathbf{r}) = \frac{8\pi e}{\epsilon} c_b \sinh(\beta e\psi) - \frac{4\pi e}{\epsilon}(p\phi^2 - p\phi_b{}^2 e^{\beta e\psi}) \quad (5)$$

$$\frac{a^2}{6}\nabla^2\phi(\mathbf{r}) = \upsilon(\phi^3 - \phi_b{}^2\phi) + p\phi\beta e\psi \quad (6)$$

Equation 5 is a generalization of the Poisson–Boltzmann (PB) equation including the free ions as well as the charged polymers. The first term represents the salt contribution and the second term is due to the charged monomers and their counterions. Equation 6 is a generalization of the self-consistent field equation of neutral polymers, obtained within the ground state dominance approximation.[25,29] In the bulk, the potential and the polymer concentration have constant bulk values given by $\psi = 0$ and $\phi = \phi_b$, as can be seen in the above equations.

At this point some attention should be drawn to the approximations involved in obtaining the two above equations. The PB equation (5) describes the electrostatic interactions at a mean-field level. It has been quite successful in describing numerous systems of charged surfaces immersed in ionic solutions (e.g., colloidal suspensions). However, it does not include ion–ion correlations which are especially important for multivalent ions at high electrostatic potentials. For more details, see, e.g., ref 30. Another effect which is not included in eq 5 is the steric repulsion between small ions due to their finite size. The PB equation can be generalized to include this interaction as well.[31–33] However, here we assume that the size of the free ions is small enough and does not play a major role in the adsorption process.

Several approximations are employed to derive the SCF equation (6). Introducing the polymer order parameter $\phi(\mathbf{r})$ instead of the individual coordinates of the monomers along the polymer chains is an important technical tool. It facilitates the calculation of average polymer concentration profiles in adsorption processes. Just as with neutral polymers, the drawback of this approach is that more specific characteristics of the chain statistics are averaged out. We note that recently it was possible to extend the continuum approach (beyond ground state dominance) and to include the statistics of loop and tail sections of neutral chains close to surfaces.[34] Another inherent assumption of eq 6 is that the charged chains remain flexible despite the stiffening nature of the Coulomb interactions. For short length scales such a flexibility persists, although the exact dependence of the persistence length on the charged polymer parameters is still a matter of debate.[35]

Although the mean-field equations 5 and 6 are somewhat restrictive, they contain much of the physics and should be regarded as a first step toward a more elaborated calculation where the effects of ionic and monomer correlations can be included in a systematic way.

B. Two Interacting Surfaces. The interaction of two charged surfaces in a solution containing only small ions (electrolyte) without charged polymers is well established within the framework of the PB equation.[36] The electrostatic interaction between two identically charged surfaces is found to be repulsive within this mean-field-like theory.[37] However, the addition of polyelectrolytes to the solution changes the picture in a subtle way. Experiments[5–13] show that polyelectrolytes reduce this repulsion and might even cause mutual attraction between the two surfaces.

For simplicity, the surfaces are taken as flat, infinite in extent, homogeneous, and parallel to each other in order that the physical quantities will depend only on the position x between the surfaces (see Figure 1). The effect of the surfaces is introduced through the boundary conditions on the polymer order parameter $\phi(x)$ and the electrostatic potential $\psi(x)$. In this work, both surfaces are assumed to be kept at the same constant potential,

$$\psi|_s = \psi_s \tag{7}$$

and no monomers are adsorbed on the surfaces

$$\phi|_s = 0 \tag{8}$$

We have chosen these boundary conditions for numerical convenience. Note that the second boundary condition effectively introduces a short-range repulsion from the surface. Other boundary conditions could have been considered as well. For example, if a fixed surface charge σ is assumed then the electrostatic boundary condition would include the electric field $\psi'|_s = -4\pi\sigma/\epsilon$. In real systems neither the surface potential nor the surface charge are fixed. The choice of one or another is only an approximation whose quality depends on the details of the experimental system. Similarly, for the polymer boundary conditions one could consider an adsorbing surface[38] instead of the nonadsorbing one.

Given these boundary conditions, the PB and self-consistent field equations (5, 6) uniquely determine $\psi(x)$ and $\phi(x)$. However, experiments usually probe global properties such as the amount of monomers adsorbed per unit area or the intersurface forces.

The total amount of monomers (per unit area) between the two surfaces $\Gamma(w)$ can be easily calculated from the polymer concentration profile since

$$\Gamma(w) = \int_{-w/2}^{w/2} \phi^2(x) \, dx \tag{9}$$

A related measure for the strength of the adsorption is the average monomer concentration divided by the bulk concentration

$$\left\langle \frac{\phi^2}{\phi_b^2} \right\rangle = \frac{1}{w} \int_{-w/2}^{w/2} \frac{\phi^2(x)}{\phi_b^2} \, dx = \frac{\Gamma(w)}{w\phi_b^2} \tag{10}$$

The latter quantity relates to the strength of the adsorption only at small distances. As demonstrated by the numerical examples below, at larger distances, Γ saturates at a constant value and the average concentration decreases as $1/w$.

In addition, it is of interest to calculate the total amount of charge (per unit area) carried by the adsorbed polymers, $\sigma_p(w) = pe\Gamma(w)$, as compared to the induced charge density on one surface $\sigma_s(w) = -(\epsilon/4\pi)\psi'|_s$. The latter depends on the intersurface distance as we have chosen to work with constant surface potentials rather than constant surface charges.

The adsorption of polyelectrolytes strongly affects the intersurface interactions and forces. The excess free energy per unit area for two surfaces at a distance w apart can be calculated from the profiles of $\phi(x)$ and $\psi(x)$:

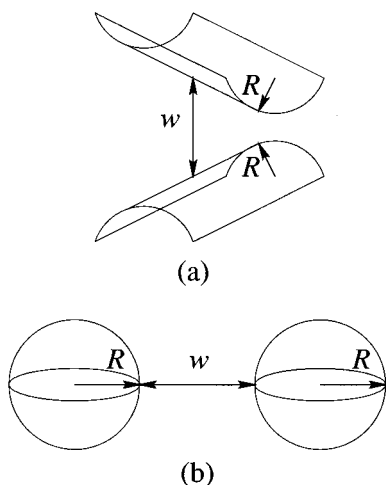$$\Delta F(w) = \int_{-w/2}^{w/2} f[\phi(x), \psi(x)] \, dx - 2F_1 \tag{11}$$

where $f(x)$ was introduced in eqs 1–4 and $F(w \to \infty) = 2F_1$ is the free energy of two isolated surfaces at infinite separation.

The variation of this free energy with respect to the intersurface distance w gives the intersurface pressure (or force per unit area).

$$\Pi(w) = -\frac{\delta(\Delta F)}{\delta w} \tag{12}$$

When the system is symmetric about the midplane $x = 0$, $\psi'(0) = \phi'(0) = 0$ and it can be shown that

$$\Pi(w) = -f(x=0) \tag{13}$$

Effect of Polyelectrolyte Adsorption

J. Phys. Chem. B, Vol. 103, No. 24, 1999 **5045**

(a)

(b)

Figure 2. (a) Two half cylinders with a 90° tilt between the axes, as used in the surface force apparatus to measure intersurface forces. The radii R of the cylinders are of the order of $1-2$ cm, while w ranges down to a few angstroms. (b) Two spheres of radii R at a distance w. Typically, colloidal suspensions contain particles whose radii are of a few micrometers down to hundreds of angstroms, while the stability is determined by the balance of forces at much smaller distances.

where $f(x=0)$ is the free energy density (per unit volume) at the midplane. Substituting $f(x=0)$ yields

$$\beta\Pi(w) = -p\phi^2(0)y(0) - \frac{1}{2}v(\phi^2(0) - \phi_b^2)^2 + p\phi_b^2[e^{y(0)} - 1] + 2c_b[\cosh(y(0)) - 1] \quad (14)$$

where $y(0) = \beta e\psi(0)$ is the reduced electrostatic potential at the symmetry plane ($x = 0$). The above expression is obtained by inserting the equilibrium (Boltzmann) distribution of the small ions $c^\pm = c_b^\pm \exp(\mp\beta e\psi)$ back into the free energy, eqs 2-4. Indeed, for neutral polymers, $\beta\Pi = -(1/2)v(\phi^2(0) - \phi_b^2)^2 < 0$ and the intersurface forces are attractive.[39] For adsorbing surfaces, this can be attributed to the elasticity of polymer chains confined between the two surfaces. On the other hand, in the absence of polymer the forces are purely repulsive $\beta\Pi = 2c_b[\cosh(y(0)) - 1] > 0$.

We note that eq 14 can be put in the form of a generalized contact theorem by integrating once the profile eqs 5 and 6. The pressure can then be expressed in terms of ϕ and ψ of any point $x \in [-w/2, w/2]$:

$$\beta\Pi(w) = \frac{a^2}{6}[\phi'(x)]^2 - \frac{1}{8\pi l_B}[y'(x)]^2 - p\phi^2(x)y(x) - \frac{1}{2}v(\phi^2(x) - \phi_b^2)^2 + p\phi_b^2[e^{y(x)} - 1] + 2c_b[\cosh(y(x)) - 1] \quad (15)$$

where $l_B = e^2/(\epsilon k_B T)$ is the Bjerrum length (equal to about 7 Å for aqueous solutions at room temperature) and $y(x) = \beta e\psi(x)$. Equations 12-15 for the force are valid for the planar geometry (Figure 1). In some experiments[13] where the disjoining pressure of thin liquid films is measured, the two surfaces are indeed parallel to each other and $\Pi(w)$ is measured directly. However, most experiments[5-12] use the surface force apparatus[4] where the force Π_R is measured between two cylindrical surfaces of radii R with a 90° tilt between their major axes (see Figure 2a). At small distances compared with the cylinder radius, $w \ll R$, the Derjaguin approximation[36] relates the measured force to the *excess free energy* (as given by eq 11) and *not* to its derivative (as given by eqs 12 and 13).

$$\frac{\Pi_R(w)}{R} = 2\pi\Delta F(w) \quad (16)$$

For clarity purposes, we denote the force per unit area acting between two infinite flat surfaces as $\Pi(w)$ (eqs 12 and 13) and the absolute force acting between two cross cylinders as $\Pi_R(w)$.

The Derjaguin approximation can also be used to calculate the interaction between two spheres of radii R at small distances $w \ll R$ as is the case for colloidal suspensions, Figure 2b. The intercolloidal force is related to the interaction free energy of two flat surfaces but with a different numerical factor:

$$\frac{\Pi_R(w)}{R} = \pi\Delta F(w) \quad (17)$$

III. Numerical Results

A. Low Salt Concentration. *Concentration Profiles.* To solve the mean-field equations (eqs 5 and 6), we use a minimal squares scheme in which the spacing between the two surfaces is divided into $N \approx 100$ intervals. An error functional which sums the squares of the local errors in eqs 5 and 6 is minimized with respect to the values of ϕ and ψ at the discrete grid points, under the constraint of the boundary conditions (eqs 7 and 8).

Typical solutions are presented in Figure 3. The polymer is positively charged ($p = 1$) and attracted to nonadsorbing surfaces held at a constant negative potential ($\psi_s < 0$). Here we focus on the weakly screened limit (low salinity). The effect of screening can be estimated by comparing the intersurface separation w with the Debye-Hückel screening length κ_s^{-1} defined by $\kappa_s^2 = 8\pi l_B c_b$. At low salt concentration, $\kappa_s^{-1} \gg w/2$, screening is weak and plays only a minor role, whereas at high salt concentration, $\kappa_s^{-1} \ll w/2$, screening strongly reduces the Coulomb interactions in the adsorbed layer. In Figure 3, the solution contains a small amount of monovalent salt ($c_b = 1$ mM). This yields an electrostatic screening length $\kappa_s^{-1} \simeq 100$ Å larger than the intersurface distance which varies between 10 and 40 Å.

In Figure 3a, the reduced electrostatic potential $y(x) = \beta e\psi(x)$ is plotted as a function of the position x between the two surfaces. The reduced monomer concentration $\phi^2(x)/\phi_b^2$ is shown in Figure 3b. Despite the fact that the surface potential is not very high, $y_s = -2.0$ corresponding to $\psi_s \simeq -50$ mV, the adsorption is quite strong and the monomer concentration in the gap between the two surfaces can increase by 3 orders of magnitude above its bulk value. The adsorption here is purely electrostatic since the only source of attraction is due to the electrostatic boundary conditions. A neutral polymer will not adsorb at all in these conditions.

At small intersurface distances, the adsorbed polymers form a single layer extending from one surface to the other and the potential is negative everywhere in the gap. As the surfaces are drawn away from each other, first the amount of adsorbed polymer grows rapidly and then the adsorbed layer separates into two distinct layers near the two surfaces. In the central region, the potential changes sign and becomes positive and the concentration of negative ions is larger than that of positive ions. As expected from charge neutrality, the charge densities of the polymer and small ions in the solution exactly balance the surface charges. However, since the amount of salt in this case is extremely low, it is mainly the polymer charge that balances the surface one (see Figure 5).
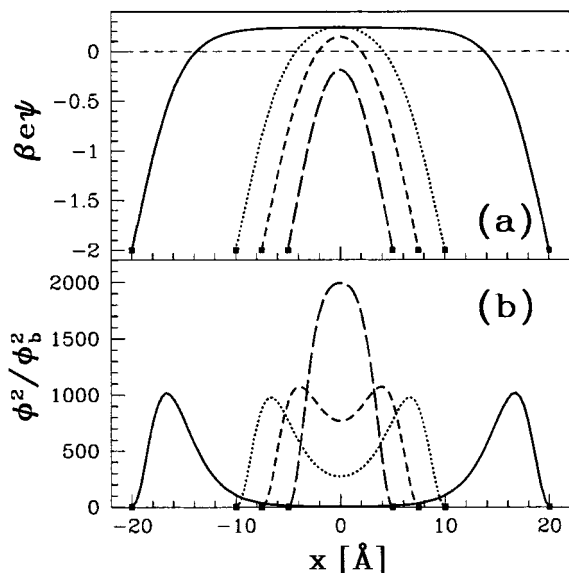
Figure 3. Profiles of (a) the reduced electrostatic potential $y = \beta e \psi$ and (b) the reduced monomer concentration ϕ^2/ϕ_b^2 as functions of the position x between the two surfaces. The profiles were obtained by solving numerically the differential equations (eqs 5 and 6) for several intersurface distances. For comparison, the different profiles are plotted on the same axis so that all midplanes ($x = 0$) coincide. The surfaces are placed at different distances from the midplane, and their positions are indicated by the filled squares. In the numerical examples in Figures 3–11, we assume the following physical parameters. The polymer concentration is $\phi_b^2 = 10^{-6}$ Å^{-3} with an effective monomer length $a = 5$ Å and excluded volume parameter $v = 50$ Å^3. It is immersed in an aqueous solution ($\epsilon = 80$) at room temperature ($T = 300$ K) and the surfaces are kept at a constant potential $y_s = \beta e \psi_s = -2$. In addition, in the current figure, the polymer charge fraction $p = 1$ and the salt concentration $c_b = 1$ mM. The different curves correspond to separations of $w = 40$ Å (solid curve); $w = 20$ Å (dots); $w = 15$ Å (short dashes), and $w = 10$ Å (long dashes).

At yet larger distances ($w > 20$ Å for the physical parameters of Figure 3), the two adsorbed layers do not change any more. This occurs when the intersurface distance w is larger than twice the width of the adsorbed layers. The two surfaces are almost decoupled, and single surface adsorption is recovered. The polymer concentration between the two adsorbed layers is small and comparable to the bulk concentration. As long as the screening length κ_s^{-1} is larger than the distance w, the electrostatic potential is nearly a constant (e.g., $y \simeq 0.2$ in Figure 3). At even larger distances, $w > \kappa_s^{-1}$, the effect of screening will show up and the midplane potential will gradually decay to zero.

Polyelectrolyte Adsorption. In Figure 4a, the total amount of monomers (per unit area) adsorbed between the two surfaces $\Gamma(w)$ is plotted as a function of the intersurface distance w for two charge fractions $p = 1$ (solid curve) and $p = 0.2$ (dashed curve). Similarly, in Figure 4b the average reduced monomer concentration $\langle \phi^2/\phi_b^2 \rangle$ is plotted as a function of w. Three regimes can be distinguished in accord with the findings presented on Figures 3 and 4; at very short distances ($w \simeq 5$ Å), the confinement of the polymer to a narrow slit competes with the electrostatic attraction of the charged monomers to the surface and avoids strong adsorption. The polymer is not expelled totally from the gap between the two surfaces, but its concentration is of the order of the bulk concentration.

As the surfaces are taken further apart, the adsorption increases rapidly until it reaches its maximal value. At this point, the average concentration can be 3 orders of magnitude higher than the bulk concentration. At larger distances, the two surfaces
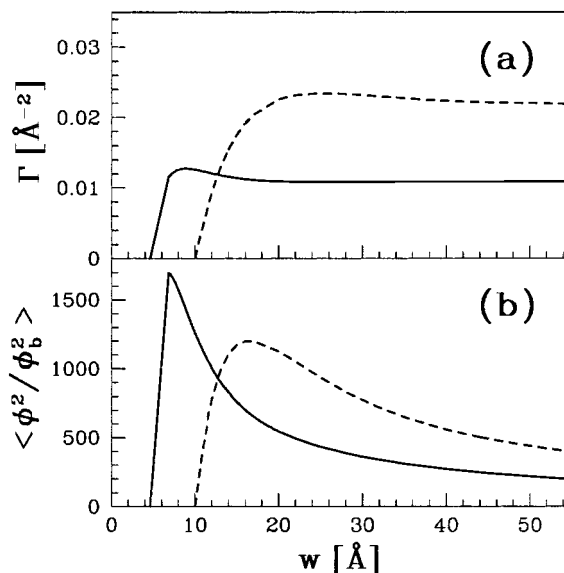

Figure 4. Adsorption of polyelectrolytes in a low-salt solution between two charged surfaces for two different polymer charge fractions: (a) total amount of monomers adsorbed between the surfaces per unit area Γ; (b) the average reduced monomer concentration $\langle \phi^2/\phi_b^2 \rangle$ as a function of the intersurface distance w. The salt concentration is $c_b = 10^{-6}$ M. The different curves correspond to charge fractions of $p = 1$ (solid curve) and $p = 0.2$ (dashed curve).

decouple from each other and the adsorbed amount decreases toward a saturation value. At this stage, the system can be described as two independent layers adsorbing onto the two surfaces. The saturation value of Γ is approximately twice the adsorbed amount to a single surface $\Gamma(w \rightarrow \infty) = 2\Gamma_1$. In a preceding work,[26] we investigated adsorption onto a single surface and have shown that in the low-salt limit $\Gamma_1 \approx 1/\sqrt{p}$. This behavior is a result of two competing interactions: (i) the electrostatic attraction of the charged monomers to the surface which is proportional to p; (ii) the Coulomb repulsion between charged monomers in the adsorbed layer which is proportional to p^2. For strong polyelectrolytes, the latter interaction dominates and the adsorbed amount Γ_1 increases as the fractional charge p decreases. This scaling behavior is in accord with the saturated values of Figure 4a.
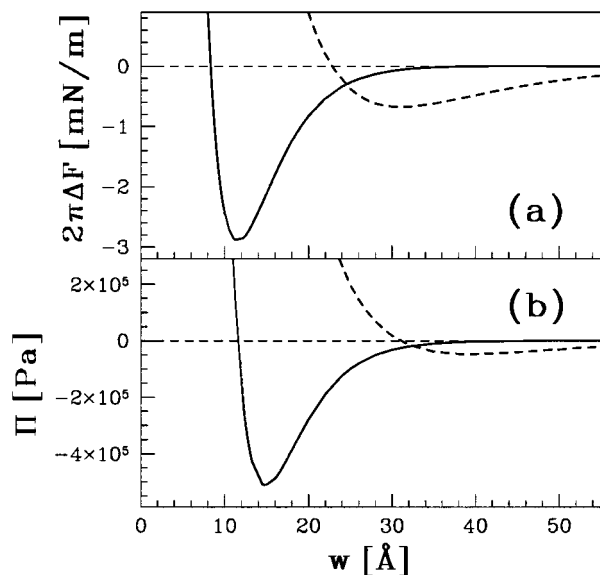
In Figure 5, the charge densities per unit area are plotted as functions of the distance w for the same sets of values as in Figure 4. Using the single surface results, we verify that indeed in the saturated regime of large intersurface separations $\sigma_p(\infty) = 2pe\Gamma_1 \simeq \sqrt{p}$. Another observation which can be made from Figure 5 is that the two charge densities almost balance each other. In the low-salt limit, these charge densities must cancel each other since the amount of salt is too small to play any significant role in neutralizing the solution.

Free Energies and Forces. In Figure 6, intersurface force profiles are presented for $c_b = 10^{-6}$ M, corresponding to $\kappa_s^{-1} \simeq 3000$ Å, and for two values of the polymer charge fraction p. In Figure 6a, the excess free energy per unit area $2\pi\Delta F(w)$, eq 11, which is the physical quantity measured in SFA experiments, is plotted as a function of the intersurface distance w. In Figure 6b, the force per unit area $\Pi(w)$, eq 12, acting between flat surfaces is plotted as a function of the distance. This force can be measured directly in disjoining pressure experiments of thin films.[13]

The two surfaces strongly repel each other at short distances and attract at larger ones. Note that for small ions such attraction is not present within the PB continuum theory. For polymer
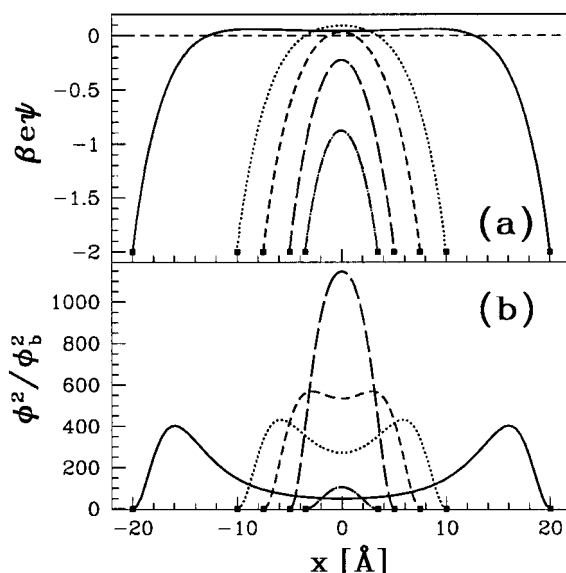
Effect of Polyelectrolyte Adsorption

J. Phys. Chem. B, Vol. 103, No. 24, 1999 **5047**
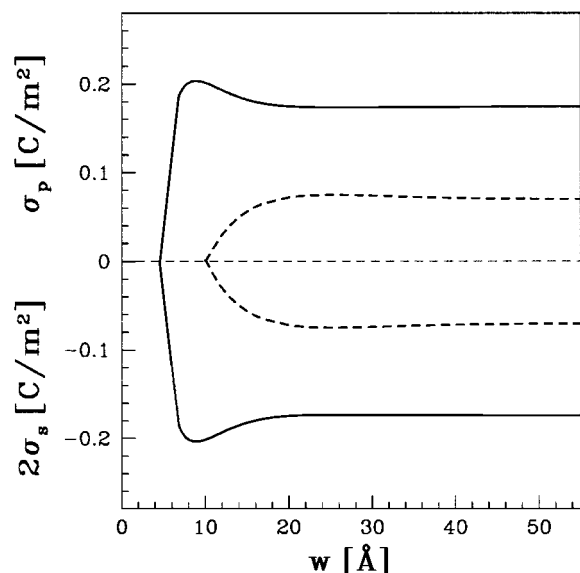
Figure 5. Charge densities per unit area as a function of the intersurface distance w. The two positive (upper) curves correspond to the total amount of polymer charge adsorbed between the two surfaces per unit area $\sigma_p \equiv pe\Gamma$. The two negative (lower) curves correspond to the induced surface charge density on both surfaces, $2\sigma_s$. The contribution of the small ions to the charge density is not displayed. The physical parameters and notations are the same as in Figure 4.

Figure 7. Profiles of (a) the reduced electrostatic potential $y = \beta e\psi$ and (b) the reduced monomer concentration ϕ^2/ϕ_b^2 as a function of the position x between the two surfaces. Same physical values and notations as in Figure 3 except for a much higher value for the salt concentration, $c_b = 1$ M. The different curves correspond to separations of $w = 40$ Å (solid curve), $w = 20$ Å (dots), $w = 15$ Å (short dashes), $w = 10$ Å (long dashes), and $w = 7$ Å (dots and long dashes).

Figure 6. Intersurface interactions for polyelectrolytes between two surfaces held at a constant potential and in a low salt solution. (a) The excess free energy per unit area $2\pi\Delta F$ as a function of the intersurface distance w. The factor 2π is used in order to enable direct comparison with SFA measurements (see eq 16). (b) The force per unit area Π between the two surfaces as a function of the intersurface distance w. The physical parameters and notations are the same as in Figure 4.

chains, the lack of translational entropy as well as the large correlation length ξ enhance the effective attraction between the surfaces at short separations. As the charge fraction is lowered, the attraction becomes weaker and the length scale of the attraction increases. These two effects can be explained by simple arguments which are presented in section IV. Attractive interactions have been observed experimentally[8] and were attributed to "bridging" of chains between the surfaces, a mechanism that exists in our approach whenever $w \lesssim \xi$.

A secondary repulsion appears at large distances but is too weak to be shown on a linear scale in our plots. However, this

secondary repulsion can be made quite pronounced, in particular when the polymer surface excess is fixed at a large value. This is further discussed in section V.

B. High Salt Concentration. *Concentration Profiles.* At high salt concentration, the screening length κ_s^{-1} is smaller than the intersurface separation w. The effect of screening on the concentration profiles is demonstrated in Figures 7 and 8, where a strong polyelectrolyte ($p = 1$) is adsorbed from a solution containing large amounts of salt, $c_b = 1$ M, for which the screening length is $\kappa_s^{-1} = 3$ Å. In Figure 7, the reduced electrostatic potential and the reduced monomer concentration are plotted as a function of the position x for a range of intersurface distances w.

As a result of screening, the attraction of charged monomers to the surface is reduced considerably as compared to the low-salt limit and the total amount of adsorbed polymer is approximately half. Despite the weaker adsorption, the qualitative behavior is similar. At short distances ($w \lesssim 15$ Å in Figure 7b), a single adsorbed layer exists between the two surfaces. At intermediate distances (15 Å $\lesssim w \lesssim 40$ Å), this layer separates into two strongly interacting layers and at larger distances ($w \gtrsim 40$ Å) the two layers decouple from each other and only weakly interact with each other.

When the separation is large ($w \gtrsim 15$ Å in Figure 7), the adsorption is strong enough so that the charged polymer overcompensates the surface charges. To explain the mechanism of charge overcompensation, we plot in Figure 8a the concentration profiles of the polymer and the small ions and in Figure 8b the potential profile for $w = 40$ Å. The points $y = 0$, $y' = 0$ and $y'' = 0$ are marked on Figure 8b, and they separate between four spatial regions. The closest to the surface is the region where $y < 0$, and it is dominated by the positive ion adsorption.
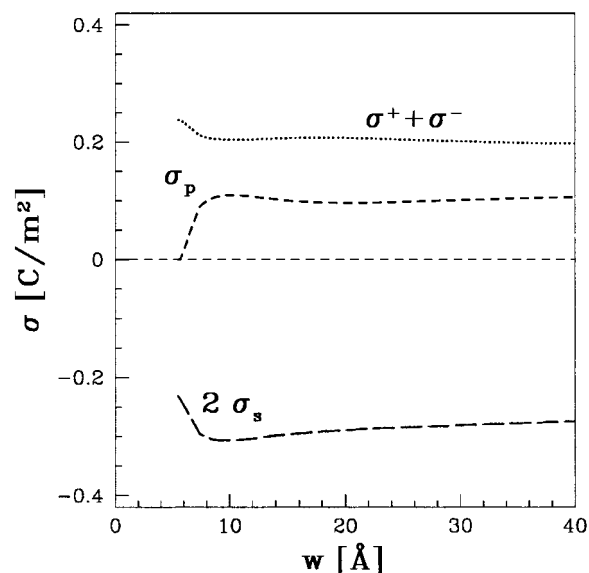
In the next two regions, the potential is positive while its curvature is negative. Since the concentration of the small ions follows a Boltzmann distribution, $c^\pm(\mathbf{r}) = c_b^\pm \exp(\mp y)$, the concentration of small negative ions c^- exceeds that of the positive ions c^+. From the Poisson equation, we know that a
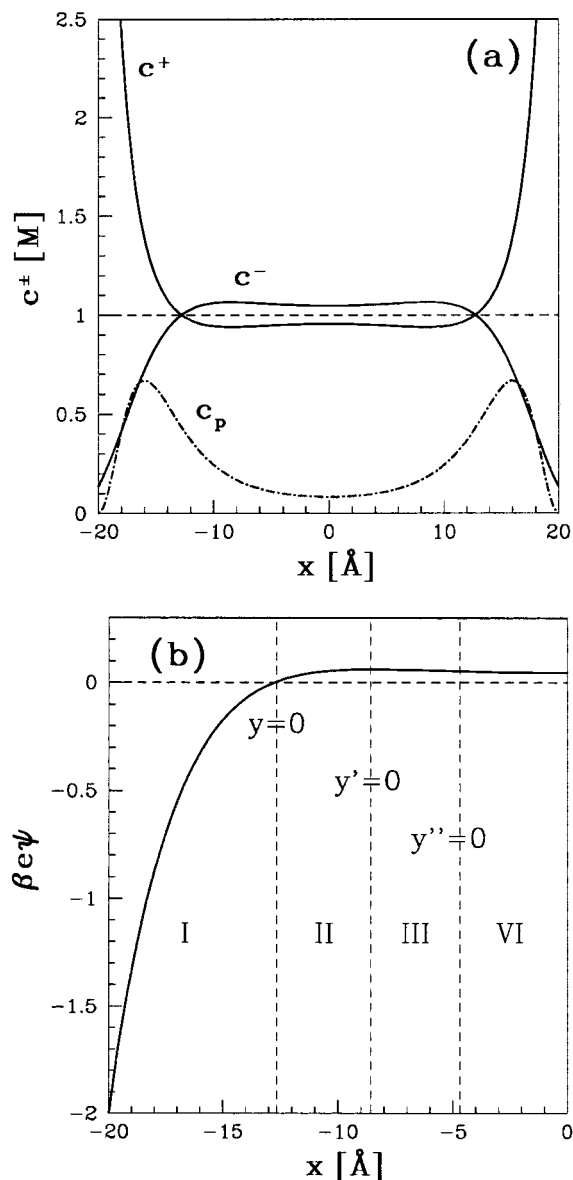
Figure 8. (a) Profiles of the charge concentrations: c^+, c^-, and $c_p = p\phi_b^2$, as functions of the position x between the two surfaces for $w = 40$ Å. The reduced electrostatic potential $\beta e\psi$ between one of the surfaces and the midplane is plotted in (b). The special points $y = 0$, $y' = 0$ and $y'' = 0$ are marked.

Figure 9. Different contributions to the total charge density per unit area as a function of the intersurface distance w for highly charged polyelectrolytes ($p = 1$) in the high-salt limit ($c_b = 1$ M). The different curves correspond to twice the induced surface charge density $2\sigma_s$, the total amount of polymer charge adsorbed between the two surfaces per unit area σ_p, and the total amount of charge carried by small ions ($\sigma^+ + \sigma^-$).

negative y'' corresponds to a positive local charge density. However, since the polymer concentration is larger than the net charge density of the small ions, $c^+ - c^-$, it is clear that the polymer adsorption is the dominant one in these two regions. These two regions are separated by the point where the electric field $E(x) = -\psi'(x)$ changes sign. Integrating the Poisson equation from the surface to this point, it can be easily shown that this sign reversal is due to an overcompensation of the surface charges. This is due to the presence of charged polymers and does not appear in the regular PB formalism for small ions (regular electrolytes). Physically, charged monomers which adsorb close to the surface are connected to other monomers which reside at some larger distance. In our model, the polymer chains resist fluctuations on length scales smaller than the correlation length ξ of the polymers and thus overcompensate the surface charges.

In the central and fourth region, the curvature itself changes sign. The negative net charge coming from the small ions exceeds that of the polymer charges. As the surface charges

are overcompensated by monomers and ions closer to the surface, the excess of negative small ions in the central region ensures an overall charge neutrality.

Note that at small separations (e.g., $w = 10$ Å in Figure 7) the potential is negative everywhere and the concentration of positive ions exceeds that of the negative ions everywhere within the gap, without charge overcompensation.

Polyelectrolyte Adsorption. Despite the effect of screening, the adsorption of strongly charged polyelectrolytes is strong, as can be seen in Figure 7b. The reason is that screening has two competing effects. On one hand, it reduces the attraction of charged monomers to the surface which is the driving force for adsorption. On the other hand, screening also reduces the monomer−monomer Coulomb repulsion between adsorbed monomers, thus allowing for more charges to accumulate near the surface. Hence, despite the fact that the range of the electrostatic interaction is reduced considerably, the average polymer concentration near the surface can be high (as long as p is not too small).

In contrast with the low-salt regime, here the small ions play an important role in balancing the surface charges. In Figure 9, the different contributions to the charge densities per unit area are plotted as a function of the distance w. These are the (induced) surface charge density on the two surfaces $2\sigma_s$, the total amount of polymer charges σ_p (per unit area) adsorbed between the two surfaces, and the total amount of charge carried by small ions $\sigma^+ + \sigma^-$. At short distances, $w \lesssim 6$ Å, the polymer contribution is small and the main contribution to the charge density is that of the small ions. This distance can also be regarded as a lower cutoff to the continuum theory employed here since the monomer size we employed is of the same order of magnitude ($a = 5$ Å).

When the surfaces are taken further apart, the polymer contribution first increases and then saturates to a constant value. This saturation occurs when the two adsorbing surfaces decouple from each other, and two distinct adsorbed layers build up on each of the surfaces. Unlike the low-salt case where the contribution of the small ions is negligible and the charged

Effect of Polyelectrolyte Adsorption

J. Phys. Chem. B, Vol. 103, No. 24, 1999 **5049**
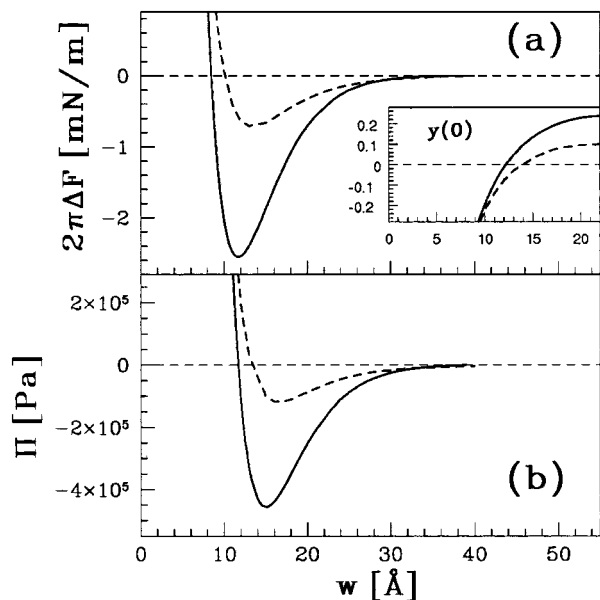
Figure 10. Intersurface interactions for highly charged polyelectrolytes ($p = 1$) at high salt concentration. (a) The excess free energy per unit area $2\pi\Delta F$ and (b) the force per unit area Π between the two surfaces as function of the intersurface distance w. The salt concentration is $c_b = 0.1$ M (solid curve) and $c_b = 1$ M (dashed curve). The inset shows the midplane values of the reduced electrostatic potential $y(0)$ as a function of w.

Figure 11. Intersurface interactions for weakly charged polyelectrolytes ($p = 0.1$) at high salt concentration. (a) The excess free energy per unit area $2\pi\Delta F$ and (b) the force per unit area Π between the two surfaces as function of the intersurface distance w. The salt concentration is $c_b = 1$ M (solid curve) and $c_b = 0.25$ M (dots).
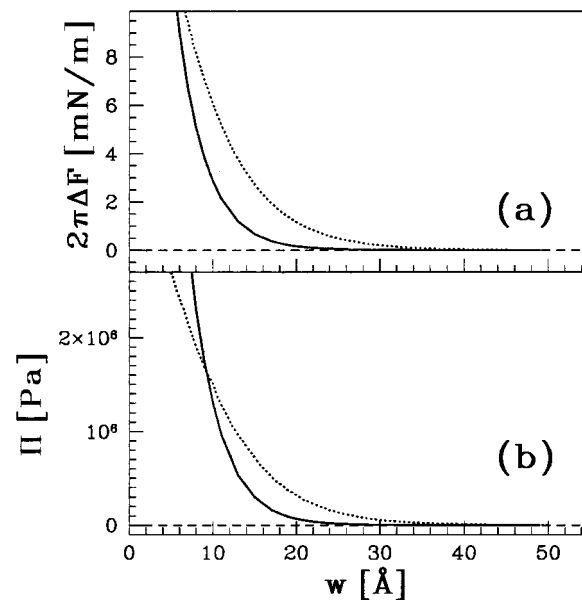
polymers dominate the charge density, in the high-salt regime the contributions of the small ions and the polymer are comparable in magnitude. For example, in Figure 9, the polymer contributes about one-third of the charge density (per unit area) between the surfaces while the small ions contribute the other two-thirds.

Free Energies and Forces. Screening has a pronounced effect on the intersurface forces as can be seen in Figure 10, where the intersurface forces are plotted as a function of the distance for a strong polyelectrolyte ($p = 1$) at two values of high salt concentration, $c_b = 0.1$ M and 1 M. The general behavior here is similar to the low-salt case as is seen in Figure 6. As the amount of salt increases, the adsorption is reduced because of the electrolyte screening and the attractive forces become substantially weaker. Similar effects were also observed experimentally in SFA experiments.[8,11]

Since the forces are related to the midplane values of ψ and ϕ (eq 12), it is of interest to study the midplane values of the potential, $\psi(0)$. In the inset of Figure 10, the midplane value of the reduced electrostatic potential $y(0) = \beta e\psi(0)$ is plotted as a function of the intersurface distance for the same profiles that are used in the calculation of the forces. As can be seen also in Figures 3 and 7, the midplane potential is negative at short distances, changes sign to become positive, and finally decays to zero. The intersurface force changes from repulsion to attraction at about the same distance where the midplane electrostatic potential changes sign. This observation can be explained by examining the various contributions to the local free energy at the midplane, eqs 2–4. At the midplane, the squared gradient terms in ϕ and ψ vanish. In addition, for strong polyelectrolytes the excluded volume and chemical potential terms are very small. The force $\Pi(w) = -f(x=0)$ is dominated by two terms:

$$\beta\Pi \simeq -p\phi^2(0)y(0) + 2c_b[\cosh(y(0)) - 1] \quad (18)$$

The first term is the contribution of the charged monomers

and changes sign when $y(0)$ changes sign. The second is the (repulsive) osmotic pressure of the small ions and is proportional to $y^2(0)$ at small values of $y(0)$. It is clear from the above that, as long as the midplane potential is small enough, $y(0) \ll p\phi^2(0)/c_b$, the pressure is governed by the first term and will change sign from attraction to repulsion when $y(0)$ changes sign. It now follows that for a positively charged polymer, negative (positive) midplane potentials lead to repulsion (attraction) in agreement with Figure 10.

Weak polyelectrolytes ($p \ll 1$) do not adsorb as much as strong polyelectrolytes. The attractive forces are much weaker and are easily overpowered by the double layer repulsion of the small ions. Such an example is presented in Figure 11, where the intersurface forces are calculated for a low charge fraction ($p = 0.1$) at two high salt concentrations $c_b = 0.25$ M and $c_b = 1$ M. In contrast with the case of strong polyelectrolytes, here the forces are repulsive over the whole distance range and decay on a length scale of κ_s^{-1}.

IV. Scaling Regimes

The fundamental difficulty in studying polyelectrolytes is due to the competition between short-range interactions such as the chain elasticity and excluded volume interactions and the long-range electrostatic interactions. In a previous work,[26] we have studied polyelectrolyte adsorption to a single surface by separating the two competing length scales: (i) the adsorption length, D, which characterizes the width of the adsorbed layer; (ii) the electrostatic screening length $\kappa_s^{-1} = (8\pi l_B c_b)^{-1/2}$ assuming that $c_b \gg p\phi_b^2$. The screening length depends on the salt concentration, while the adsorption length depends on both electrostatic and nonelectrostatic properties.

The two length scales can be separated in two limits: (i) the low-salt regime $D \ll \kappa_s^{-1}$; (ii) the high-salt regime $D \gg \kappa_s^{-1}$. The difference between the two regimes is the range of the electrostatic interactions. The main assumption in this approach is that the polymer profile near a single flat surface can be written in the form

$$\phi(x) = \sqrt{C}\, h\!\left(\frac{x}{D}\right) \tag{19}$$

where $h(z)$ is a dimensionless function normalized to unity at its maximum and C sets the scale of polymer adsorption. The free energy can then be expressed in terms of D and C while the exact form of $h(z)$ affects only the numerical prefactors. Minimization of the free energy with respect to D and C gives the single surface adsorption length D_1 and the concentration scale C_1.

When two surfaces interact with each other, the single surface profile is affected by the presence of the other surface. As a result, the shape of the profile changes with the separation w as demonstrated in Figures 3 and 7. For example, at short distances, the profile varies monotonically between the surface and the midplane, while at larger distances it becomes nonmonotonic, until finally the two surfaces decouple from each other and the adsorption to each surface reduces to the single surface behavior.

As in the single surface case, it is advantageous to separate the different length scales. First, we compare the single surface adsorption length D_1 with the intersurface separation w. At large separations $w/2 \gg D_1$, the surfaces interact weakly and the polyelectrolytes recover the single surface profiles. On the other hand, at short intersurface distances $w/2 \ll D_1$, the gap is too small for the polyelectrolytes to follow the single surface profile. In this limit, the relevant length scale (eq 19) is just $D = w/2$, since $w/2$ serves as a lower cutoff for D. When $w/2$ increases so that $w/2 \simeq D_1$, the profile becomes more complex and our main assumption is no longer valid. Nevertheless, as demonstrated below, this simplified picture reproduces the main features that characterize the intersurface forces in those short distances, $w/2 \le D_1$.

Furthermore, the effect of screening can be taken into account by separating the screening length from the two other length scales. Two opposite limits are considered: (i) the low salt regime $\kappa_s^{-1} \gg D_1$ and (ii) the high salt regime $\kappa_s^{-1} \ll D_1$.

A. Low-Salt Regime: $\kappa_s^{-1} \gg D_1$. In the low-salt regime, the screening length is much larger than the width of the adsorbed layer and the effect of the small ions on the structure of the adsorbed layer can be neglected. This assumption amounts to neglecting the entropic contribution to the free energy $f_{ions}(\mathbf{r})$ (eq 3) and the electrostatic energies of the small ions in $f_{el}(\mathbf{r})$ (eq 4).

Large Distances: $w/2 \gg D_1$. At large distances $w/2 \gg D_1$, the two surfaces are only weakly coupled. The structure of the adsorbed layer near each of the two surfaces reduces to the single surface profile, and the "decorated" surfaces interact through a weak double layer interaction. In the limit of large distances and low-salt conditions, one needs to address the question of the relative size of $w/2$ and κ_s^{-1} as both lengths are large.

The free energy of an isolated adsorbing surface can be approximated by[26]

$$\beta F_p^{(1)}(C,D) = \alpha_1 \frac{a^2}{6D}\, C - \alpha_2 p|y_s|CD + 4\pi\beta_1 l_B p^2 C^2 D^3 + $$
$$\frac{1}{2}\beta_2 \nu C^2 D \tag{20}$$

The first term is the polymer elastic energy (or connectivity) term, the second term is the electrostatic interaction of the monomers with the surface, and the third term is the Coulomb repulsion between the adsorbed monomers. The electrostatic terms can be derived by integrating the interaction of every pair of charged layers at distances x and x' from the surface, with

charge densities (per unit area) $d\sigma = pe\phi^2(x)\,dx$ and $d\sigma' = pe\phi^2(x')\,dx'$, respectively. Finally, the last term is the excluded volume term and will be neglected here since at low salt concentration its contribution is important only for extremely weakly charged polyelectrolytes.

The coefficients α_1, α_2, β_1, and β_2 are numerical prefactors which depend on the exact shape of the dimensionless scaling function $h(z)$. These coefficients can be explicitly calculated for a specific profile by integrating the Poisson equation without taking into account the small ion contributions. For the simplest monotonic profile, namely a linear profile $h_1(z) = z$ for $0 \le z \le 1$ and $h_1(z) = 0$ for $z > 1$, we get $\alpha_1 = 1$, $\alpha_2 = 1/3$, $\beta_1 = 1/14$, and $\beta_2 = 1/5$. For a nonmonotonic parabolic profile, $h_2(z) = 4z(1 - z)$ for $0 \le z \le 1$ and $h_2(z) = 0$ elsewhere, we get $\alpha_1 = 16/3$, $\alpha_2 = 8/15$, $\beta_1 \simeq 1/9$, and $\beta_2 \simeq 2/5$. Another profile which we consider is an intermediate profile of the form $h_3(z; \eta) = 4z(\eta - z)/\eta^2$ for $0 \le z \le 1$ and $h_3(z) = 0$ elsewhere, where η is a parameter. This profile is nonmonotonic and has a finite value at $z = 1$, which corresponds to the symmetry plane between the two surfaces. Furthermore, the special cases $\eta \gg 1$ and $\eta = 1$ reduce to the simple linear and parabolic profiles $h_1(z)$ and $h_2(z)$, respectively. The parabolic profile $h_2(z)$ is a good choice for an isolated adsorbing surface in contact with a bulk of low concentration, whereas $h_1(z)$ describes better interacting surfaces at small separation. The third profile $h_3(z; \eta)$ can be regarded as intermediate between the other two. We stress that our scaling results do not depend on the specific shape of the profile $h(z)$. Only the numerical prefactors will change.

The single surface free energy (eq 20) can be minimized with respect to both D and C along the same lines as was done in ref 26. This yields a length scale D_1 characterizing the adsorption onto a single surface

$$D_1 \simeq \frac{a}{p^{1/2}|y_s|^{1/2}} \tag{21}$$

and a concentration scale

$$C_1 \simeq \frac{|y_s|^2}{l_B a^2} \tag{22}$$

In the low-salt limit, screening effects can be neglected as long as the screening length κ_s^{-1} is much larger than the adsorption length D_1, which can also be viewed as the local correlation length of the polymer. This condition limits the low-salt regime to

$$c_b \ll \frac{p|y_s|}{l_B a^2} \tag{23}$$

Inserting the above expressions back in the free energy gives the single surface free energy (up to numerical factors),

$$\beta F_p^{(1)} \simeq -\frac{p^{1/2}|y_s|^{5/2}}{l_B a} \tag{24}$$

At distances larger than the adsorbed layer $x > D_1$ the amount of polyelectrolytes is small and comparable to its (low) bulk value. Since $p\phi_b^2 \ll c_b$ (even in the low-salt limit), the interaction at large distances can be simplified. The system can be regarded as a solution containing electrolytes only (no polyelectrolytes) between two *effective* surfaces positioned at the edge of the adsorbed layers $x = \pm(w/2 - D_1)$. The effective intersurface distance is now $w_{eff} = w - 2D_1$, and each surface

Effect of Polyelectrolyte Adsorption

J. Phys. Chem. B, Vol. 103, No. 24, 1999 **5051**

is kept at a (reduced) potential $y_D = \beta e \psi_D$ which is much smaller in magnitude than the original surface potential $|\psi_D| \ll |\psi_s|$.

In the absence of polyelectrolytes in the effective gap, the electrostatic potential between two charged surfaces can be obtained by solving the PB equation:[36]

$$\nabla^2 \psi(\mathbf{r}) = \frac{8\pi e}{\epsilon} c_b \sinh(\beta e \psi) \qquad (25)$$

The above equation can be obtained from eq 5 in the no polyelectrolyte limit. After the differential equation has been solved with the appropriate boundary conditions (namely, $\psi = \psi_D$), the repulsive free energies and intersurface forces can be calculated. In particular, eq 25 can be solved analytically in the weakly coupled regime, $\kappa_s^{-1} \ll w_{eff}/2$, yielding the following expressions for the repulsive intersurface forces:

$$\beta \Delta F_{el} = 64 c_b \kappa_s^{-1} \tanh^2(y_D/4) e^{-\kappa_s w_{eff}} \simeq 4 c_b \kappa_s^{-1} y_D^2 e^{-\kappa_s w_{eff}} \qquad (26)$$

$$\beta \Pi_{el} = 64 c_b \tanh^2(y_D/4) e^{-\kappa_s w_{eff}} \simeq 4 c_b y_D^2 e^{-\kappa_s w_{eff}} \qquad (27)$$

Other electrostatic regimes exist in which eq 25 can be solved analytically. Those regimes lie beyond the scope of the present study because the polymer adsorbed layer reduces substantially the electric potential. Unfortunately, our model is too simple to give an accurate estimate of y_D which is a local property. For this purpose more refined models are required.

Short Distances: $w/2 \ll D_1 \ll \kappa_s^{-1}$. At short separations $w/2 \ll D_1 \ll \kappa_s^{-1}$ the relevant length scale in eq 19 is $w/2$ instead of D. Consequently, and due to the planar symmetry of the system, the polymer contribution to the free energy can be written as $F_p(C,w) = 2F_p^{(1)}(C,D=w/2)$ where $F_p^{(1)}(C,D)$ is the single surface free energy (eq 20).

The free energy is minimized now only with respect to C leading to

$$C \simeq \frac{|y_s|}{l_B p} \frac{w^2 - w_{min}^2}{w^4} \qquad (28)$$

where $w_{min}^2 = 2\alpha_1 a^2/(3\alpha_2 p |y_s|)$. The condition that C be positive limits the validity of eq 28 to distances larger than a minimal distance w_{min}, while at shorter distances $C = 0$ and the polymers are depleted from the region between the surfaces. We estimate $w_{min} \simeq 0.2 D_1$, and so eq 28 is valid in the range $0.1 D_1 < w/2 < D_1$.[40]
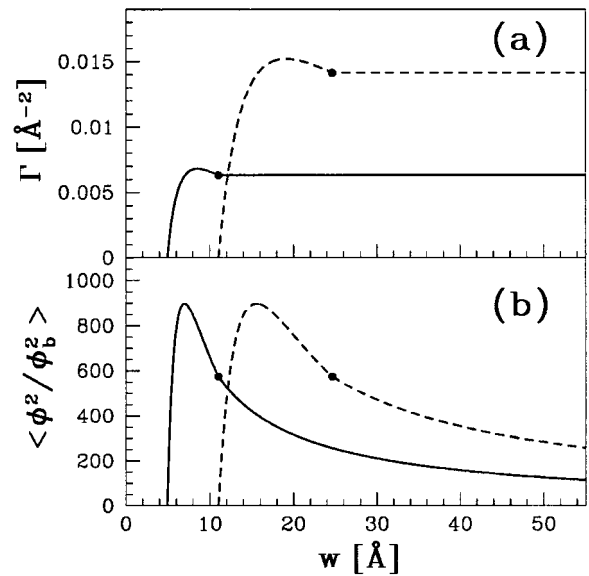
The total amount of monomers (per unit area) adsorbed between the two surfaces is directly related to C and C_1.

$$\Gamma(w) = \int_{-w/2}^{w/2} \phi^2(x)\, dx = \begin{cases} 0 & w < w_{min} \\ \alpha_2 w C(w) & w_{min} < w < 2D_1 \\ 2\alpha_2 D_1 C_1 & 2D_1 < w \end{cases} \qquad (29)$$

Similarly, the average reduced monomer concentration is given by

$$\left\langle \frac{\phi^2}{\phi_b^2} \right\rangle = \frac{\Gamma(w)}{w\phi_b^2} = \begin{cases} 0 & w < w_{min} \\ \alpha_2 C(w)/\phi_b^2 & w_{min} < w < 2D_1 \\ 2\alpha_2 D_1 C_1/w\phi_b^2 & 2D_1 < w \end{cases} \qquad (30)$$

The adsorption properties $\Gamma(w)$ and $\langle \phi^2/\phi_b^2 \rangle$ are plotted in Figure 12 as a function of the intersurface distance w for the same physical values of Figure 4. Our results agree qualitatively

Figure 12. Adsorption of polyelectrolytes in the low-salt regime as calculated from eqs 29 and 30. (a) Total amount of monomers adsorbed between the surfaces per unit area Γ, and (b) the average reduced monomer concentration $\langle \phi^2/\phi_b^2 \rangle$ as function of the intersurface distance w. The physical values and notations are the same as in Figure 4. The numerical prefactors of the intermediate profile $h_3(z,\eta)$ with $\eta = 3/2$ were used in the calculation. The vertical lines denote the distance where $w = 2D_1$.

with the numerical results of Figure 4 and reproduce the three different adsorption regimes.

Inserting the above expression for C (eq 28) back into the free energy yields

$$\beta F_p \simeq -\frac{|y_s|^2}{l_B} \frac{(w^2 - w_{min}^2)^2}{w^5} \qquad (31)$$

for $w_{min} < w < 2D_1$. At distances shorter than w_{min}, the polyelectrolyte is depleted from the gap and the intersurface force is dominated by electrostatic repulsion.[41]

The intersurface force Π_p is readily obtained by differentiating the free energy F_p with respect to w.

$$\beta \Pi_p = -\frac{\delta(\beta F_p)}{\delta w} \simeq -\frac{|y_s|^2}{l_B} \frac{(w^2 - w_{min}^2)(w^2 - 5w_{min}^2)}{w^6} \qquad (32)$$

A quantitative comparison with the numerical results is shown in Figure 13 where the physical parameters are the same as in Figure 6. In Figure 13, the polymer contribution to the excess free energy $\Delta F_p(w) = F_p(w) - 2F_p^{(1)}$ and to the intersurface force Π_p are plotted as functions of the intersurface separation w. The single surface free energy $F_p^{(1)}$ is calculated from eq 24. Only small separations $w < 2D_1$ are shown in the figure. For $w > 2D_1$ the shape of the intersurface profile is more complex, and we do not have scaling arguments relating the polymer profiles with the force. However, we expect the polymer contribution to be small. Comparing Figure 13 with Figure 6, we note that our scaling results (the characteristic length scale as well as the characteristic force) are in good agreement with the numerical results for several p values.

B. High-Salt Regime: $\kappa_s^{-1} \ll D_1$. In the high-salt regime, the screening length is much smaller than the adsorption length D_1. The Coulomb interactions between the charged monomers and the surface and between the monomers themselves decay exponentially with the Debye–Hückel screening length κ_s^{-1}.
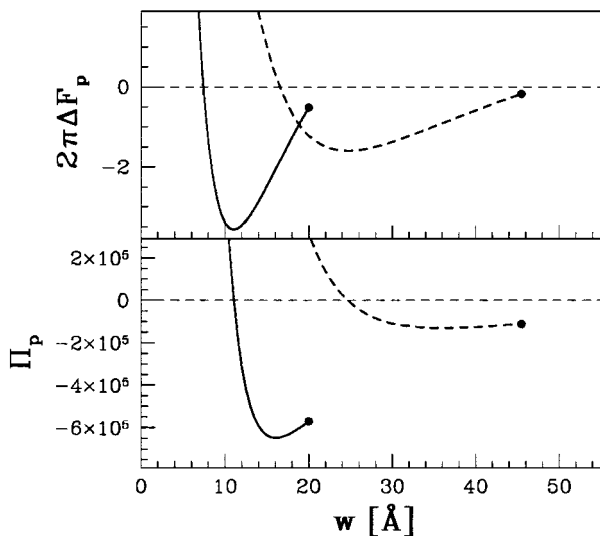
Figure 13. Polyelectrolyte contribution to (a) the interaction free energy, $2\pi\Delta F_p$ (eq 31) and (b) the intersurface force, Π_p (eq 32), in the low-salt regime as function of the intersurface separation w. Same physical values, notations, and units as in Figure 6. The numerical prefactors of the intermediate profile $h_3(z,\eta)$ with $\eta = 3/2$ were used in the calculation of the interaction free energy and forces, and the numerical prefactors of the parabolic profile were used in the calculation of the single surface free energies. Solid line $p = 1$; dashed line $p = 0.2$.

Our calculation is based on estimating the polymer contribution to the forces as mediated by the small ions. One should bear in mind that the contribution of the small ions to the forces is no longer negligible and can explain the discrepancy between the numerical (exact) and the scaling results. It is hard to get an analytical estimate to the small ions contribution because their concentration depends on the polymer profile via the electric potential.

Large Distance: $w/2 \gg D_1$. The free energy (eq 20) can be generalized by introducing κ_s^{-1} as a cutoff on the range of the electrostatic interactions (similar to what was done in ref 26 for the single surface case):

$$\beta F_p(C,D) = \alpha_1 \frac{a^2}{6D} C - \alpha_2 p|y_s|C\kappa_s^{-1} +$$
$$4\pi\beta_1 l_B p^2 \kappa_s^{-2} C^2 D + \frac{1}{2}\beta_2 v C^2 D \quad (33)$$

The electrostatic cutoff appears in two places. In the second term, only the first layers up to a distance κ_s^{-1} from the surface interact with the surface charges. In the third term, each layer interacts only with its neighboring layers in the range of κ_s^{-1}. The numerical values of the prefactors α_1, α_2, β_1, and β_2 can in principle be different from the low-salt values. However, since the prefactors are only used in Figure 14 to demonstrate the qualitative behavior, we will arbitrarily set their values to be the same as in the low-salt regime.
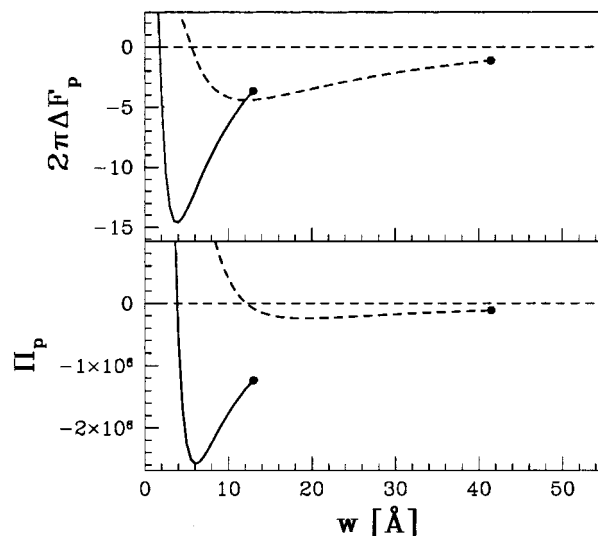
Minimizing eq 33 with respect to D and C yields

$$D_1 \simeq \frac{\kappa_s a^2}{p|y_s|} \approx \frac{c_b^{1/2}}{p} \quad (34)$$

and

$$C_1 \simeq \frac{p^2|y_s|^2/(\kappa_s a)^2}{\beta_1 p^2/c_b + \beta_2 v} \quad (35)$$

which are now also functions of the salt concentration c_b or,

Figure 14. Polyelectrolyte contribution to (a) the interaction free energy, $2\pi\Delta F_p$ (eq 39) and (b) the intersurface force, Π_p (eq 40), in the high-salt regime as a function of the intersurface separation w. Same physical values, notations, and units as in Figure 10. The numerical prefactors of the intermediate profile $h_3(z,\eta)$ with $\eta = 3/2$ were used in the calculation of the interaction free energy and forces, and the numerical prefactors of the parabolic profile were used in the calculation of the single surface free energies. Solid line $c_b = 0.1$ M; dashed line $c_b = 1$ M.

equivalently, $\kappa_s = (8\pi l_B c_b)^{1/2}$. The condition that the screening length is much smaller than the adsorption length amounts to

$$c_b \gg \frac{p|y_s|}{8\pi l_B a^2} \quad (36)$$

in agreement with the boundary of the low-salt regime (eq 36).

The single surface free energy is now

$$\beta F_p^{(1)} \simeq -\frac{p^3|y_s|^3\kappa_s^{-3}}{(\beta_1 p^2/c_b + \beta_2 v)a^2} \quad (37)$$

As in the low-salt regime, the two adsorbed layers interact electrostatically. However, since the screening length is much shorter than the adsorption length in the high-salt regime, this interaction decays quite rapidly. We note that the high-salt regime can be further divided into two subregimes depending on the ratio of the two terms in the denominator of C_1 and $F_p^{(1)}$ as was discussed in ref 26.

Short Distances: $w/2 \ll D_1$. At short distances, the relevant length scale in the free energy eq 33 is $w/2$ instead of D (as in the low-salt regime). The free energy can be minimized with respect to C yielding

$$C \simeq \frac{p|y_s|\kappa_s^{-1}}{\beta_1 p^2/c_b + \beta_2 v}\frac{w - w_{min}}{w^2} \quad (38)$$

where $w_{min} = \alpha_1\kappa_s a^2/(3\alpha_2 p|y_s|)$. As in the low-salt case, C is positive only for $w > w_{min} \simeq 0.2D_1$. At smaller separations, the polyelectrolytes are depleted from the gap and the intersurface force is dominated by the electrostatic repulsion. We also note that the validity of eq 33 requires that $w \gg 2\kappa_s^{-1}$.

The polymer free energy of interaction is now

$$\beta F_p \simeq -\frac{p^2|y_s|^2\kappa_s^{-2}}{\beta_1 p^2/c_b + \beta_2 v}\frac{(w - w_{min})^2}{w^3} \quad (39)$$

Effect of Polyelectrolyte Adsorption

J. Phys. Chem. B, Vol. 103, No. 24, 1999 **5053**

and the intersurface force

$$\beta\Pi_p \simeq -\frac{p^2|y_s|^2\kappa_s^{-2}}{\beta_1 p^2/c_b + \beta_2 v}\frac{(w - w_{min})(w - 3w_{min})}{w^4} \quad (40)$$

The qualitative behavior described by eqs 39 and 40 is similar to that of the low-salt regime (eqs 31 and 32). The typical behavior for a strong polyelectrolyte is depicted in Figure 14, where the same physical parameters of Figure 10 are used. We note that the quantitative agreement between the numerical (Figure 10) and scaling (Figure 14) results is not as good as in the low-salt limit. For example, the value of the minimum in the free energy is about 3 times smaller in Figure 14 as compared with Figure 10. Also, the variation of w at this minimum with the salt concentration is weaker in the numerical results. As discussed above, the main source of discrepancy between the numerical and scaling results is the omission of the small ion contribution in the latter.

C. Discussion. To summarize our results, we present in Figure 15 a schematic diagram of the different adsorption regimes. The dashed lines mark the single surface adsorption regimes in terms of the charge fraction p and the salt concentration c_b. Three adsorption regimes can be distinguished: (i) the low-salt regime $c_b \ll p|y_s|/8\pi l_B a^2$; (ii) the first high-salt (HS I) regime $c_b \gg p|y_s|/8\pi l_B a^2$ with weak polyelectrolytes $p^2 \ll vc_b$; (iii) the second high-salt (HS II) regime $c_b \gg p|y_s|/8\pi l_B a^2$ with strong polyelectrolytes $p^2 \gg vc_b$.

The shaded area in Figure 15 marks the region in parameter space where the polymer contribution to the intersurface interaction is comparable to or larger than the pure electrostatic contribution. The shaded area includes the low-salt regime, a large portion of the HS II (high salt/strong polyelectrolyte) regime and a small portion of the HS I (high salt/weak polyelectrolyte) regime. The exact crossover lines depend, of course, on the numerical coefficients which are not included in our approximations. Nevertheless, the qualitative picture can be deduced from the diagram.

The different behaviors (as depicted previously) can be demonstrated with the help of this diagram. The filled circles in the low-salt regime mark the graphs of Figure 6 and are well within the shaded area. The filled squares on the right border of the diagram (at $p = 1$) correspond to the graphs of Figure 10 representing strong polyelectrolytes in the high salt regime. At higher salt concentration, the system is closer to the boundary of the shaded area and the polymer attraction is weaker. Finally, when the ionic strength is high enough, the attractive contribution is too weak to be observed. Weak polyelectrolytes in the high-salt regime belong to the top left side of the diagram outside of the shaded area. In this regime, the electrolyte dominates the intersurface forces which are purely repulsive, as is indeed the case for the force curves of Figure 11. These curves are represented in Figure 15 by filled triangles.

In the following, we briefly summarize our findings in the different adsorption regimes. In section VI, the findings are compared with experimental works which are reported in the literature.

Low-Salt Regime. In the low-salt regime, the Debye−Hückel screening length is much larger than the width of the adsorbed layer. As a result, the electrostatic interactions of the charged monomers with the surfaces and their interactions with other monomers are unscreened. This leads to strong adsorption as can be seen from the numerical results shown in Figures 3 and 4 and from the scaling results (eqs 29 and 30) shown in Figure 12. In addition, since the bulk concentration of the salt and
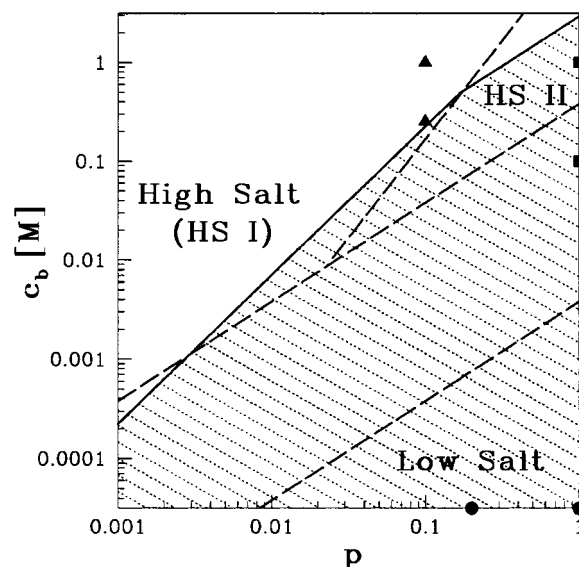
Figure 15. Schematic diagram of the different regimes as a function of the charge fraction p and the salt concentration c_b. Three regimes can be distinguished: (i) the low-salt regime $D_1 \ll \kappa_s^{-1}$; (ii) the high-salt regime (HS I) $D_1 \gg \kappa_s^{-1}$ for weak polyelectrolytes $p \ll (c_b v)^{1/2}$; (iii) the high-salt regime (HS II) $D_1 \gg \kappa_s^{-1}$ for strong polyelectrolytes $p \gg (c_b v)^{1/2}$. The shaded area denotes the region where the polymer interactions are strong enough so that intersurface attraction can be observed. The filled circles correspond to the numerical force−distance profiles of Figure 6, the filled squares correspond to the numerical profiles of Figure 10, and the filled triangles to the profiles of Figure 11.

counterions, c_b and $p\phi_b^2$, respectively, is small, the charge density in the solution between the two surfaces is mainly due to the charged monomers. This is demonstrated in Figure 5, where it is shown that the surface charges are balanced by the charged monomers.

At large distances, the adsorbed polymer forms two distinct layers on the two surfaces. The amount of polymer adsorbed between the two surfaces saturates to a constant value (Figure 4) which is approximately twice the single surface adsorbed amount. As discussed in a preceding work,[26] the width of the single surface adsorbed layer D_1 and the single surface adsorbed amount Γ_1 both scale as $p^{-1/2}$. The dependence on p is due to the balance between the attraction of the monomers to the surface which is proportional to p and the monomer−monomer Coulomb repulsion which is proportional to p^2. The fact that the adsorbed amount decreases when the polymer charge increases reflects the energy barrier for bringing a large amount of charged monomers to the vicinity of the charged surface.

The two layers start to overlap when the intersurface distance is about twice the width of the single surface adsorbed layer $w \simeq 2D_1$. Below this distance, the adsorbed amount slightly increases (Figure 4) and the two surfaces strongly attract each other (Figure 6). Our scaling approach recovers the increase in the adsorbed amount (eq 29 and Figure 12) and the attraction of the two surfaces (eqs 31 and 32 and Figure 13). The magnitude of the polymer contribution to the interaction free energy scales as

$$\beta\Delta F_p \approx \frac{p^{1/2}|y_s|^{1/2}}{l_B a} \quad (41)$$

This energy scale should be compared with the electrostatic interaction energy which scales as

$$\beta\Delta F_{el} \approx c_b\kappa_s^{-1}|y_s|^2 \quad (42)$$

5054 *J. Phys. Chem. B, Vol. 103, No. 24, 1999*

Borukhov et al.

The condition that ΔF_p is at least comparable to ΔF_{el} limits the salt concentration to

$$c_b < \frac{p|y_s|}{l_B a^2} \qquad (43)$$

in agreement with the boundary of the low-salt regime (eq 23).

If the intersurface distance is further reduced, the entropy loss due to the confinement of the polymer to a narrow slit pushes the polymer out of the gap between the two surfaces. This can be seen from the numerical results (Figure 4) and also from eq 28, where w_{min} is the minimal distance below which the polymer is compelled to leave the gap.

High Salt Regime. In the high-salt regime, the Debye−Hückel screening length κ_s^{-1} is much smaller than the width of the adsorbed layer. As a result, the range of the electrostatic interactions is much shorter and each charged monomers interacts only with monomers at a distance smaller than κ_s^{-1}.

The limiting behavior at large distances depends strongly on the charge fraction p. For weak polyelectrolytes where p is small (regime HS I), the monomer−monomer Coulomb repulsion which is proportional to p^2 is negligible and the single surface adsorbed amount Γ_1 scales as $p/c_b^{1/2}$. On the other hand, for strong polyelectrolytes where p is large (regime HS II) the monomer−monomer Coulomb repulsion is dominant and the single surface adsorbed amount Γ_1 scales as $c_b^{1/2}/p$. The latter behavior is similar to that of the low-salt regime with a different p dependence. At higher salt concentration, the adsorbed amount increases as the monomer−monomer Coulomb repulsion at the adsorbed layer is screened out.

In the high-salt case, the contribution of the small ions to the charge density cannot be neglected. As seen in Figure 9, about two-thirds of the surface charge are balanced by small ions and only one-third by charged monomers. Another interesting aspect of the interplay between charged polymer chains and small ions is the spatial distribution of charges between the two surfaces.

The polyelectrolytes are strongly adsorbed on the surface resulting in a sign reversal of the potential: it is negative at the surface and becomes positive at a distance of 6−7 Å. In order that the system will be overall neutral, the central region between the two surfaces has an excess of negative ions as seen in Figure 8. At short distances (less than 12−14 Å), this effect disappears and the potential is negative everywhere in the gap. As seen from Figure 10 and eq 18 the sign reversal of the midplane potential $y(x=0)$ is accompanied by a sign reversal in the intersurface force $\Pi(w)$.

When the two surfaces are brought closer together, $w < 2D_1$, these layers start to overlap (See Figure 7) and the adsorbed amount slightly increases. At this separation, strong polyelectrolytes induce strong attraction between the two surfaces (Figure 10). Indeed, as was discussed before, since D_1 is the correlation length of the polymer, for $w < 2D_1$ bridging effects occur and are responsible for the attraction. The polymer contribution to the attraction can be estimated from our scaling approach to be

$$\beta\Delta F_p \approx \frac{p^3|y_s|^3\kappa_s^{-3}}{(\beta_1 p^2/c_b + \beta_2 v)a^2} \qquad (44)$$

Following the low-salt discussion, we compare this interaction with the electrostatic interaction energy (eq 42). For weak polyelectrolytes $p^2 \ll v c_b$ (regime HS I), the polymer contribution dominates for

$$c_b^2 < \frac{p^3|y_s|}{l_B a^2 v} \qquad (45)$$

while for strong polyelectrolytes $p^2 \gg v c_b$ the polymer contribution is dominant at low salt concentration.

$$c_b \ll \frac{p|y_s|}{l_B a^2} \qquad (46)$$

At very short distances $w < w_{min}$ (eq 38), the polymer is depleted from within the gap as can be also seen in Figure 9.

V. Irreversible Adsorption

So far we have assumed that the adsorbed layer is in thermodynamic equilibrium with a bulk reservoir. Hence, the total amount of adsorbed monomers can vary and is determined by the free energy minimization (eqs 1−4). However, in physical systems the energetic barrier for detaching an adsorbed chain from the surface can be much larger than the thermal energy $k_B T$. As a result the relaxation times toward equilibrium can be much larger than the experimental time scales, and the amount of adsorbed monomers can be taken as fixed.

The experimental procedure for irreversible adsorption is obtained in the following way. First, the two surfaces are held at large distance from one another as they are immersed in a polyelectrolyte solution. The solution is then washed out so that only a polymer surface excess $\Gamma_0/2$ remains attached to each surface. Third, the two surfaces are brought together assuming that the surface excess remains constant in the process. The possibility of polymer exchange with the reservoir is excluded. For simplicity, we limit ourselves to the low-salt case. The results can be generalized to the high-salt case. In principle, the state of the system is determined by minimizing the free energy (eqs 1−4) under the constraint that

$$\int_{-w/2}^{w/2} \phi^2(x)\, dx = \Gamma_0 \qquad (47)$$

where Γ_0 is the predetermined value of the amount of polymer between the surfaces. Note that our procedure, although forbidding exchange of polymers with the reservoir, assumes full equilibration between the two adsorbing plates. This is not the case in most experimental setups.

The constraint (eq 47) can be introduced through a Lagrange multiplier λ replacing the chemical potential term in F so that the functional to be minimized becomes

$$\beta\tilde{F} = \beta F - \lambda \left(\int_{-w/2}^{w/2} \phi^2(x)\, dx - \Gamma_0 \right) \qquad (48)$$

The self-consistent field equation now reads

$$\frac{a^2}{6}\nabla^2\phi(\mathbf{r}) = v\phi^3 + p\phi\beta e\psi - \lambda\phi \qquad (49)$$

where we have omitted the chemical potential term since now the adsorbed layer does not exchange polymer chains with the reservoir. The modified PB equation (eq 5) is not affected by the irreversibility of the adsorption process, since the counterions are still free to exchange between the reservoir and the adsorbed layer.

Equations 5 and 49 are solved under the constraint of eq 47 where λ is adjusted to give the desired value of Γ_0. Typical force profiles calculated numerically are presented in Figure 16a, where the free energy $2\pi\Delta F$ is plotted as a function of the

Effect of Polyelectrolyte Adsorption

J. Phys. Chem. B, Vol. 103, No. 24, 1999 **5055**
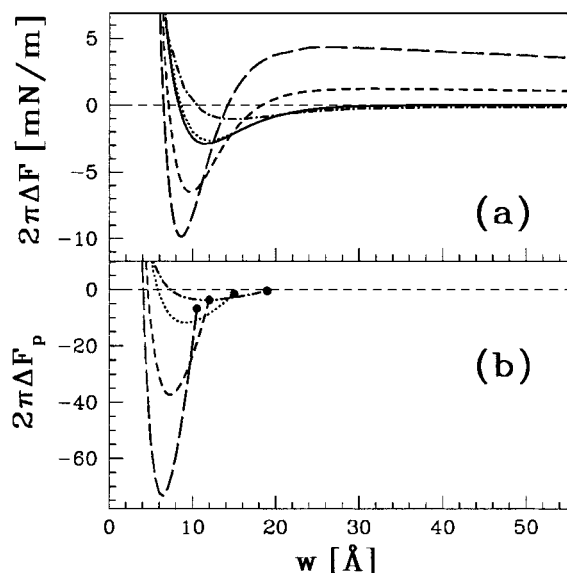
Figure 16. The effect of irreversible polyelectrolyte adsorption on the interaction free energy. The excess free energy per unit area $2\pi\Delta F$ is plotted as a function of the intersurface distance w. The graphs in (a) were obtained by solving numerically the mean-field equations 5 and 49 under the constraint of eq 47. The solid curve corresponds to the equilibrium interaction free energies and is the same as the solid curve of Figure 6. The four curves were obtained for the same physical values as in Figure 5 with $p = 1$, while the total amount of adsorbed monomers was kept at a constant value Γ_0. The different curves correspond to $\Gamma_0 = \Gamma_{sat} = 0.011$ Å^{-2} (dots), $\Gamma_0 = 2\Gamma_{sat}$ (small dashes), $\Gamma_0 = 3\Gamma_{sat}$ (long dashes), and $\Gamma_0 = \Gamma_{sat}/2$ (dot−dash line). The graphs in (b) were calculated from the analytical expressions of the scaling approach (eqs 52 and 53).

intersurface distance w. For comparison, we plot on the same graph the equilibrium free energy (solid curve) of Figure 6. The dotted curve was calculated for the same physical values with the additional constraint that the total amount of monomers adsorbed between the surfaces is fixed to the equilibrium value of single surface adsorption (or equivalently two surfaces held at large distances). This value is defined as Γ_{sat}. As can be seen from Figure 4a, for $p = 1$, $\Gamma_{sat} = 0.011$ Å^{-2}.

The free energy difference between the solid and dotted curves is quite small and appears only at short distances when the adsorbed amount in true equilibrium starts to deviate from its saturated value (see also Figure 4). Different values of Γ_0 are shown on Figure 16a. For low values of Γ_0 (e.g., $\Gamma_0 = \Gamma_{sat}/2$), the attraction is weaker, while for higher values (e.g., $\Gamma_0 = 2\Gamma_{sat}$), the attraction is much stronger.

To understand better this behavior, we return to the scaling approximation where we consider first the case of irreversible adsorption on a *single* surface. We assume that a fixed amount $\Gamma = \Gamma_0/2$ is adsorbed to the surface. Since the adsorbed amount Γ is related to the length scale D and the concentration scale C through $\Gamma = \alpha_2 CD$, it is possible to express C in terms of D and thus the free energy (eq 20) in terms of D and Γ_0. Neglecting the excluded volume term, equation 20 now becomes

$$\beta F_p^{(1)}(\Gamma_0, D) = \frac{\alpha_1}{12\alpha_2}\frac{a^2}{D^2}\Gamma_0 - \frac{1}{2}p|y_s|\Gamma_0 + \frac{\pi\beta_1}{\alpha_2^2}l_B p^2 \Gamma_0^2 D \quad (50)$$

Minimization of the free energy with respect to D yields

$$D_{irr} \simeq \left(\frac{a^2}{l_B p^2 \Gamma_0}\right)^{1/3} \quad (51)$$

Substituting D_{irr} back in the free energy gives

$$\beta F_p^{(1)} \simeq -\frac{1}{2}p|y_s|\Gamma_0 + a^{2/3}l_B^{2/3}p^{4/3}\Gamma_0^{5/3} \quad (52)$$

where we have omitted some numerical coefficients. The first term in eq 52 is simply the interaction energy of the charged monomers with the surface, while the second term is a balance between the monomer−monomer Coulomb repulsion and the chain elasticity term.

When the two surfaces are interacting with each other, we can write an explicit expression for $F_p(w)$ at small distances ($w \ll D_{ir}$) by replacing the adsorption length scale D with $w/2$. The free energy then becomes

$$\beta F_p(w) = \frac{2\alpha_1}{3\alpha_2}\frac{a^2}{w^2}\Gamma_0 - p|y_s|\Gamma_0 + \frac{\pi\beta_1}{\alpha_2^2}l_B p^2\Gamma_0^2 w \quad (53)$$

The interaction free energy is now $\Delta F_p = F_p(w) - 2F_p^{(1)}$. The surface interaction term cancels out, and we are left with three terms, two positive terms from eq 53 and a negative term from eq 52. The latter scales as $\Gamma_0^{5/3}$ and is responsible for the attraction at short distances where the third term of eq 53 becomes small. In Figure 16b, we plot the interaction free energy as calculated from eqs 52 and 53 for the same physical values as in Figure 16a. Although the numerical coefficients cannot be obtained accurately from this approach, the qualitative behavior is in accord with the numerical results.

VI. Comparison with Experiments

The experimental studies with the surface force apparatus[5−12] focus mostly on the repulsive interactions between adsorbing surfaces. Due to the limitations of the experimental technique, the attractive interactions at short distances appear as jumps in force−distance profiles. Nevertheless, some of the qualitative features can be deduced from the experiments and agree with our findings.

Luckham and Klein[5] have measured interactions between mica surfaces in the presence of poly-L-lysine, which is a strong polyelectrolyte ($p = 1$) at two different salt concentrations $c_b = 1$ mM and $c_b = 0.1$ M. The intersurface forces $\Pi_R(w)$ (eq 16) were measured at distances 50 Å $< w <$ 1200 Å. The forces were always repulsive, decaying exponentially as function of w with decay lengths comparable to the Debye−Hückel screening length κ_s^{-1}. These forces can be interpreted as the electrostatic repulsion between two adsorbed layers at distances larger than the width of a single layer (eq 26). Significant deviations were found between the first approach where the two surfaces are brought close together and subsequent decompression−compressions cycles. The amplitude of the repulsion in the latter case was strongly reduced, while the decay length of the force remained quite the same. In addition, the amount of polymer adsorbed between the two surfaces, as estimated by refractive index measurements, was much higher than that in the initial measurements. Those effects demonstrate that the adsorbed layers are not always in equilibrium and that compression might lead to strong adsorption of charged polymers. The adsorbed amount remains high when the surfaces are separated from each other due to the high energetic barrier for desorption. The reduction in the intersurface repulsion when the adsorbed amount is high is in accord with our numerical and analytical results for the case of irreversible adsorption (section V).

Marra and Hair[6] have adsorbed poly(2-vinylpyradine) (P2VP) between mica surfaces. The pH of the solution was such that the polymer was fully charged ($p = 1$) during the experiments. At low salt concentrations, the forces were repulsive at large

5056 *J. Phys. Chem. B, Vol. 103, No. 24, 1999*

Borukhov et al.

distances with an exponential decay which is consistent with the Debye−Hückel screening length. Attraction of about −7 mN/m was detected at distances between 11 and 40 Å. In the presence of 0.01 M NaCl, the magnitude of the repulsive forces increased while the attraction was reduced to −3 mN/m and shifted to distances between 25 and 80 Å. At even higher ionic strengths (0.1 M NaCl), the attraction disappeared altogether but an additional nonexponential contribution to the intersurface repulsion was detected at distances between 60 and 100 Å. These results confirm our findings that the effect of salt is to increase the adsorption length D_1 and to reduce the polymer attractive contribution to the intersurface forces.

Claesson and Ninham[7] have adsorbed chitosan, a cationic biopolymer of glucosamine segments, between mica surfaces in the presence of 0.01 wt % acetic acid. The chitosan charge fraction was controlled through the pH of the solution

$$p = \frac{10^{-(pH-pK_0)}}{1 + 10^{-(pH-pK_0)}} \tag{54}$$

where $K_0 = 10^{-pK_0} \simeq 10^{-6.5}$ is the dissociation constant of the chitosan monomers. At low pH, the polymer is fully charged and the interactions were repulsive in the first compression when the surfaces were brought into contact. A double layer repulsion was detected at large distances ($w > 100$ Å) and strong steric repulsion at shorter distances. Upon separation, attraction was detected at distances around 20−25 Å. At pH = 6.2 ($p \simeq 2/3$), the repulsive double layer interaction disappeared altogether. The disappearance of the electrostatic double layer interaction indicates that the surface charges are exactly balanced by the adsorbed polymers. Attraction was detected at distances of about 20−25 Å, and strong steric repulsion at shorter separations. At pH = 9.1 where the polymer was only weakly charged ($p \simeq 1/400$), the double layer repulsion was again the dominant interaction.

Dahlgren et al.[8] have studied the effect of salt concentration by adsorbing poly((3-methacrylamido propyl)trimethylammonium chloride) (MATPAC) between mica surfaces. Three salt concentrations were considered $c_b = 0.1$ mM, 0.01 M, and 0.1 M. The forces were repulsive at large distances and decayed exponentially with decay lengths of 170, 30, and 11 Å, respectively. The first decay length is smaller than the Debye−Hückel screening length of the corresponding salt concentration ($\kappa_s^{-1} \simeq 300$ Å) due to the contribution of the counterions. At higher salt concentrations, this contribution is negligible and the decay lengths agree with the expected screening lengths. Attractive interactions were detected at short distances of a few nanometers. The magnitude of these attractive forces decreased as the amount of salt increased in agreement with the numerical results of Figure 10.

In another work, Dahlgren et al.[9] have studied the effect of both charge fraction and salt concentration on the intersurface forces. Three different polyelectrolytes with different charge fractions p were used, MAPTAC ($p = 1$) and two copolymers AM-CMA-10 ($p = 0.1$) and AM-CMA-30 ($p = 0.3$), which were prepared using different ratios of neutral acrylamide (AM) segments and positively charged (2-acroyloxy ethyl)trimethylammonium chloride (CMA) segments. For a fixed charge fraction ($p = 0.3$), three different ionic strengths were compared: $c_b = 0.1$ mM, $c_b = 0.01$ M, and $c_b = 0.1$ M. These experiments correspond to a vertical scan in Figure 15. At the lowest ionic strength, the system is in the low-salt regime and strong attraction is detected at intermediate distances $40 < w < 100$ Å. At the next ionic strength ($c_b = 0.01$ M), the system is in the lower

part of the high-salt regime and weak attraction is still observed at distances below 60 Å. At the higher value of $c_b = 0.1$ M, no attractive interactions are observed and the electrostatic repulsions dominate the intersurface forces. For a fixed ionic strength ($c_b = 0.1$ mM), Dahlgren et al. have compared the intersurface forces for three different charge fractions: $p = 0.1$, $p = 0.3$, and $p = 1$. This set of experiments corresponds to a horizontal cut in Figure 15. At the lowest charge fraction, the repulsive interactions are dominant, while for higher values of p, attractions is observed at distances below $w \simeq 100$ Å.

Finally, the effect of ionic strength was studied separately by Dahlgren.[11] Two polyelectrolytes, poly(2-proplyionyloxy ethyl)trimethylammonium chloride) (PCMA) and MAPTAC, which have different molecular weight but the same charge fraction ($p = 1$), were studied. The monomers of these polymers are large, and therefore the regime boundaries in Figure 15 should be shifted to lower salt concentrations. Dahlgren has compared several types of multivalent salts at intermediate ionic strengths which are equivalent to $c_b = 0.1$, 0.2, 0.3, and 0.6 mM. In the higher ionic strengths (0.3 and 0.6 mM), no attractive interactions were observed. However, at lower ionic strengths, attraction was observed at distances below $w \simeq 120$ Å and $w \simeq 180$ Å for $c_b = 0.1$ mM and $c_b = 0.2$ mM, respectively. The ratio between the two lengths scales is approximately $\sqrt{2} \simeq 1.4$ in agreement with the adsorption length scale in the high salt regime $D_1 \approx c_b^{1/2}$ (eq 34). Furthermore, the adhesion force was measured as $\Pi_{ad} \simeq 170$ mN/m and $\Pi_{ad} \simeq 250$ mN/m in agreement with the force scale of strong polyelectrolytes in regime HS II $F_p \approx 1/c_b^{1/2}$ (eq 44).

VII. Conclusions

In this paper, we calculated numerically concentration profiles of polyelectrolytes between two charged surfaces and studied the intersurface forces as a function of the distance between the charged surfaces. Overcompensation of surface charges by adsorbed monomers and coions was found for highly charged polymers and high salt conditions. This charge overcompensation is strongly connected to the fact that the monomer charge does not satisfy a Boltzmann distribution. Its concentration is affected by electrostatic as well as nonionic interactions. We find that the presence of charged polymer can induce reversal of intersurface forces from repulsion to attraction at short distances where the two adsorbing layers strongly overlap.

The effect of the polymer charge and ionic strength on the intersurface force is studied by means of a simple variational approach. Three main regimes are found: (i) a low-salt regime, $c_b \ll p|y_s|/8\pi l_B a^2$; (ii) a high-salt regime $c_b \gg p|y_s|/8\pi l_B a^2$ for weak polyelectrolytes $p^2 \ll \nu c_b$ (HS I); (iii) a second high-salt regime for strong polyelectrolytes $p^2 \gg \nu c_b$ (HS II).

In the low-salt regime, strong repulsion at very short distances is a result of the polymer depletion from the intersurface gap. As the distance increases to $w \approx a/p^{1/2}$, strong attraction is due to overlap of the adsorbed layers. Finally, when the intersurface separation is larger than twice the adsorption length of a single surface, the two adsorbed layers separate and repel each other electrostatically. In the HS II regime, the behavior is similar to the low-salt one, with a modified length scale of interaction given by $\kappa_s a^2/p$. On the other hand, in the HS I regime, the polyelectrolyte attractive contribution is too weak to generate a similar attraction at short distances. Consequently, the intersurface interaction is repulsive with a decay length of κ_s^{-1}.

Some of the features described above are also present in the discrete lattice model of Böhmer et al.[18] In particular, attractive interactions between equally charged surfaces were obtained numerically (Figure 9 of ref 18). This attraction was attributed

Effect of Polyelectrolyte Adsorption

J. Phys. Chem. B, Vol. 103, No. 24, 1999 **5057**

to bridging by polymer chains from one surface to the other. The lattice model contains information regarding the fine details of the polymer chains which are absent in our model. On the other hand, the continuum approach is a convenient starting point for analytical approximations such as the scaling approach presented in this work. Attractive interactions were also obtained by Podgornik[27] for the case of fixed adsorbed amount and without considering the nonlinear excluded volume interaction. For polyelectrolytes in a poor solvent, Châtellier and Joanny[28] have obtained oscillations in the polymer concentration as well as in the intersurface forces.

The model presented here takes into account the important Coulombic degrees of freedom within the framework of the PB formalism. We solve the coupled nonlinear equations for the electrostatic potential and polymer concentration which allows consistent treatment of excluded volume effects as well as strong potential and surface charges (not the linearized Debye–Hückel version). This allows us to consider cases where the Coulombic degrees of freedom are a major perturbation on the adsorption of neutral polymers.

At the same time, our approach has several limitations, some of which can be improved. The polymer chains are treated within a mean-field approximation which misses certain properties of polymer statistics such as the chain connectivity, stiffening of the persistence length, finite chain corrections, and more specific conformations of polymers close to surfaces (loops, tails, and trains).

On the other hand, the simple model we present offers a qualitative picture of polyelectrolyte chains between surfaces and suggests several scaling regimes. It can be further improved to take into account more realistic situations such as surface heterogeneities and other geometries, various charge distributions (quenched and annealed) on the chains,[24,25,42] pH effects for acidic and basic polyelectrolytes[26] as well as finite ion or monomer sizes.[31–33]

In this work, we have assumed constant surface potentials. One could also consider constant surface charges. In the low-salt limit, the behavior is expected to resemble the case of a fixed amount of adsorbed polymer since the charged monomers are the main source of charges which are able to neutralize the surface charges. In the presence of salt, this is no longer the case and the behavior can differ considerably. It would be interesting to have thorough experimental results on the effect of the charge fraction p and salt concentration c_b on the nature and magnitude of the forces and the corresponding length scales. We hope that our present work will encourage such systematic experimental studies.

References and Notes

(1) Joanny, J. F.; Leibler, L.; de Gennes, P. G. *J. Polym. Sci.* **1979**, *17*, 1073.

(2) Cabane, B.; Wong, K.; Wang, T. K.; Lafuma, F.; Duplessix, R. *Colloid Polym. Sci.* **1988**, *266*, 101.

(3) Dickinson, E.; Eriksson, L. *Adv. Coll. Interface Sci.* **1991**, *34*, 1 and references therein.

(4) Israelachvili, J.; Adams, G. E. *J. Chem. Soc., Faraday Trans. 1* **1978**, *74*, 975.

(5) Luckham, P. F.; Klein, J. *J. Chem. Soc., Faraday Trans. 1* **1984**, *80*, 865.

(6) Marra, J.; Hair, M. L. *J. Phys. Chem.* **1988**, *92*, 6044.

(7) Claesson, P. M.; Ninham, B. W. *Langmuir* **1992**, *8*, 1506.

(8) Dahlgren, M. A. G.; Waltermo, Å.; Blomberg, E.; Claesson, P. M.; Sjöström, L.; Åkesson, T.; Jönsson, B. *J. Phys. Chem.* **1993**, *97*, 11769.

(9) Dahlgren, M. A. G.; Claesson, P. M.; Audebert, R. *Nord. Pulp Pap. Res. J.* **1993**, *8*, 62.

(10) Claesson, P. M.; Dahlgren, M. A. G.; Eriksson, L. *Colloids Surf. A* **1994**, *93*, 293.

(11) Dahlgren, M. A. G. *Langmuir* **1994**, *10*, 1580.

(12) Lowack, K.; Helm, C. A. *Macromolecules* **1998**, *31*, 823.

(13) Bergeron, V.; Langevin, D.; Asnacios, A. *Langmuir* **1996**, *12*, 1550.

(14) Van der Schee, H. A.; Lyklema, J. *J. Phys. Chem.* **1984**, *88*, 6661.

(15) Papenhuijzen, J.; Van der Schee, H. A.; Fleer, G. J. *J. Colloid Interface Sci.* **1985**, *104*, 540.

(16) Evers, O. A.; Fleer, G. J.; Scheutjens, J. M. H. M.; Lyklema, J. *J. Colloid Interface Sci.* **1985**, *111*, 446.

(17) Van de Steeg, H. G. M.; Cohen Stuart, M. A.; de Keizer, A.; Bijsterbosch, B. H. *Langmuir* **1992**, *8*, 8.

(18) Böhmer, M. R.; Evers, O. A.; Scheutjens, J. M. H. M. *Macromolecules* **1990** *23*, 2288.

(19) Åkesson, T.; Woodward, C.; Jönsson B. *J. Chem. Phys.* **1989**, *91*, 2461.

(20) Granfeldt, M. K.; Jönsson, B.; Woodward, C. E. *J. Phys. Chem.* **1991**, *95*, 4819. Podgornik, R.; Åkesson, T.; Jönsson, B. *J. Chem. Phys.* **1995**, *102*, 9423.

(21) Muthukumar, M. *J. Chem. Phys.* **1987**, *86*, 7230.

(22) Varoqui, R.; Johner, A.; Elaissari, A. *J. Chem. Phys.* **1991**, *94*, 6873.

(23) Varoqui, R. *J. Phys. II (France)* **1993**, *3*, 1097.

(24) Borukhov, I.; Andelman, D.; Orland, H. *Europhys. Lett.* **1995**, *32*, 499.

(25) Borukhov, I.; Andelman, D.; Orland, H. *Eur. Phys. J. B* **1998**, *5*, 869.

(26) Borukhov, I.; Andelman, D.; Orland, H. *Macromolecules* **1998**, *31*, 1665.

(27) Podgornik, R. *J. Phys. Chem.* **1992**, *96*, 695.

(28) Châtellier, X.; Joanny, J. F. *J. Phys. II (France)* **1996**, *6*, 1669.

(29) De Gennes, P. G. *Scaling Concepts in Polymer Physics*; Cornell University: Ithaca, 1979.

(30) Kjellander, R.; Marcelja, S.; Pashley, R. M.; Quirk, J. P. *J. Chem. Phys.* **1990**, *92*, 4399.

(31) Eigen, M.; Wicke, E. *J. Phys. Chem.* **1954**, *58*, 702.

(32) Kralj-Iglic, V.; Iglic, A. *Electrotech. Rev. (Slovenia)* **1994**, *61*, 127. Kralj-Iglic, V. *Electrotech. Rev. (Slovenia)* **1995**, *62*, 104. Kralj-Iglic, V.; Iglic, A. *J. Phys. II (France)* **1996**, *6*, 477.

(33) Borukhov, I.; Andelman, D.; Orland, H. *Phys. Rev. Lett.* **1997**, *79*, 435.

(34) Semenov, A.; Joanny, J. F.; Johner, A. In *Theoretical and mathematical models in polymer research*; Grosberg, A., Ed.; Academic Press: Boston, 1998; p 37.

(35) Barrat, J. L.; Joanny, J. F. *Europhys. Lett.* **1993**, *24*, 333.

(36) For a review, see: Israelachvili, J. N. *Intermolecular and Surface Forces*, 2nd ed.; Academic Press: London, 1990. Andelman, D. In *Handbook of Biological Physics*; Lipowsky, R., Sackmann, E., Eds.; Elsevier Science B.V.: Amsterdam, 1995; Vol. 1B, p 603.

(37) Recent measurements of intersurface forces in the presence of asymmetric electrolytes (such as $CaCl_2$) and without polyelectrolytes followed by theoretical calculations using the hypernetted chain (HNC) scheme have indicated that ion correlations beyond mean field can lead to attraction of symmetric surfaces at very short separations of a few angstroms, e.g., ref 32.

(38) De Gennes, P. G. *Macromolecules* **1981**, *15*, 1637.

(39) De Gennes, P. G. *Macromolecules* **1982**, *15*, 492.

(40) Since the linear profile $h_1(z)$ is a better approximation at small distances, we use it in order to estimate the lower cutoff w_{min}, while the coefficients of the parabolic profile $h_2(z)$ are used in the calculation of the single surface adsorption length D_1.

(41) Depletion forces contribute to intersurface attraction. However, this contribution is proportional to $k_B T v \phi_b^4$ and is much smaller than the electrostatic repulsion.

(42) Raphael, E.; Joanny, J. F. *Europhys. Lett.* **1990**, *13*, 623.